UCRL 9109

UNIVERSITY OF CALIFORNIA

Ernest O. Lawrence

Radiation Laboratory

PARAMAGNETIC RESONANCE OF TETRAVALENT Pa^{231}

TWO-WEEK LOAN COPY

This is a Library Circulating Copy which may be borrowed for two weeks. For a personal retention copy, call Tech. Info. Division, Ext. 5545

DISCLAIMER

This document was prepared as an account of work sponsored by the United States Government. While this document is believed to contain correct information, neither the United States Government nor any agency thereof, nor the Regents of the University of California, nor any of their employees, makes any warranty, express or implied, or assumes any legal responsibility for the accuracy, completeness, or usefulness of any information, apparatus, product, or process disclosed, or represents that its use would not infringe privately owned rights. Reference herein to any specific commercial product, process, or service by its trade name, trademark, manufacturer, or otherwise, does not necessarily constitute or imply its endorsement, recommendation, or favoring by the United States Government or any agency thereof, or the Regents of the University of California. The views and opinions of authors expressed herein do not necessarily state or reflect those of the United States Government or any agency thereof or the Regents of the University of California.

For research and development

UCRL-9109
UC-4 Chemistry General
TID-4500 (15th Ed)

UNIVERSITY OF CALIFORNIA
Lawrence Radiation Laboratory
Berkeley, California

Contract No. W-7405-eng-48

PARAMAGNETIC RESONANCE OF TETRAVALENT Pa^{231}

Ru-Tao Kyi

(Thesis)

March 4, 1960

Printed in USA. Price $1.75. Available from the
Office of Technical Services
U. S. Department of Commerce
Washington 25, D.C.

PARAMAGNETIC RESONANCE OF TETRAVALENT Pa^{231}

Contents

Abstract 3

I. Introduction 4

II. Fundamentals of Paramagnetic Resonance

A. Resonance Pheonomena 5

B. Nuclear Interactions and Hyperfine Structure . . 6

C. Experimental Aspects 7

III. Theory of Paramagnetic Resonance[8]

A. Hamiltonian of an Ion in a Single Crystal and in the Presence of an External Magnetic Field . . . 11

B. Derivation of the Spin Hamiltonian 14

C. Ground State of a 5f' Electron Configuration in an Octahedral Crystalline Field 18

D. Ground State of a 6d' Electron in the Octahedral Crystalline Field 29

IV. Experimental Procedure

A. Isolation of Pa^{+5} in Solution from Cationic Impurities 34

B. Preparation of Solid $PaCl_4$ 37

C. Single-Crystal Preparation 44

D. Paramagnetic Resonance Measurement 46

V. Results 48

VI. Discussion 61

VII. Acknowledgments 63

VIII. References 65

PARAMAGNETIC RESONANCE OF TETRAVALENT Pa^{231}

Ru-Tao Kyi
(Thesis)

Lawrence Radiation Laboratory
University of California
Berkeley, California
March 4, 1960

ABSTRACT

The paramagnetic-resonance spectrum of tetravalent Pa^{231} has been observed in a matrix of $Cs_2 Zr Cl_6$. A melt of $Cs_2 Zr Cl_6$ was doped with ~500 μgms of anhydrous $Pa^{231} Cl_4$ and allowed to crystallize in an atmosphere of hydrogen by slow passage through a furnace. At $4^{\circ}K$ the observed resonance pattern consisted of four widely separated hyperfine components. The spectrum was isotropic to within the accuracy of the field measurements (~1/2 %). These features are interpreted as the "allowed" transitions between levels caused by the perturbation

$$\mathcal{H} = g\beta \vec{H} \cdot \vec{S} + A \vec{I} \cdot \vec{S} \quad .$$

with $S = 1/2$ and $I = 3/2$. Best fit for the data is obtained with $|g| = 1.148$ (±.005) and $|A| = 0.0529$ (±.0005) cm^{-1} no resonance was detected at $77^{\circ}K$.

The nuclear-spin assignment of 3/2 is verified. The paramagnetism can be most plausibly ascribed to a single 5f electron. A magnetically isotropic Kramer's doublet is expected to be the lowest lying as the result of the octahedral perturbation present in a Zr site. As an alternative, a $6d^1$ configuration is expected to give rise to a four-fold degenerate magnetically anisotropic level if octahedral symmetry is preserved, or an anisotropic doublet if distortion is present.

I. INTRODUCTION

On the basis of the lanthanide and actinide analogy, the first 5f electron would be expected formally to be present in the ground state of the neutral atom of thorium, atomic number 90. Spectroscopic evidence shows that the ground-state configuration of Th^0 is $6d^2 7s^2$, with no "f" electron present. Indeed the configuration $5f6d7s^2$ lies some 10^3 cm^{-1} above the ground state. In trebly ionized thorium, on the other hand the configuration 5f' is more stable by some $10^4 cm^{-1}$ than the 6d' configuration. The ground-state configuration of Pa^0 is not known, but it is to be expected that quadruply ionized protactinium would have a ground-state configuration of 5f'. However, at the beginning of the actinide series the alternative "f" and "d" configuration are of nearly equivalent energy, and the effect of chemical binding might well stabilize the "d" configuration in preference to that of "f".

This investigation was undertaken to secure experimental evidence regarding the configuration of Pa(IV) in a condensed phase.

Since electron-spin-resonance studies of the paramagnetic ions give a great deal of information about the energy states of the unpaired electrons, it is the most sensitive method to be used to study the electronic configurations. For the actinide elements, the ions U^{+3}, [1] NpO_2^{++}, [2] NpF_6 PuO_2^{++}, [3] Cm^{+4}, [4] and Am^{+3}, [5] have been studied by this method, and the result have been interpreted as due to $5f^3$, $5f^1$, $5f^2$, and $5f^6$ configurations.

Because of the difficulty in producing a thorium ion or a protactinium ion having odd electrons outside the atom core, and because of the difficulty in single-crystal growing, there is a lack of paramagnetic-resonance data on these two elements. In this thesis, the tetravalent protactinium, which posseses only one electron outside the atom core, has been studied in a single crystal diluted with a matrix of dicesium zirconium hexachloride, Cs_2ZrCl_6. The crystal has cubic symmetry. The ground states of the ion in the two cases: (a) with a 6d or (b) with a 5f electron outside the atom core in a cubic crystalline field are studied theoretically.

II. FUNDAMENTALS OF PARAMAGNETIC RESONANCE

A. Resonance Phenomena

When an ion having a resultant angular momentum and a colinear magnetic moment is placed in a constant external magnetic field H, the angular momentum vector will precess about the field direction with the angular velocity

$$\omega = g \left(\frac{e}{2mc} \right) H \tag{2.1}$$

where g is called the spectroscopic splitting factor or g factor, e and m are the electronic charge and mass, and c is the velocity of light. If a circularly polarized magnetic field is also applied, with such a sense and frequency that it rotates about H in synchronism with the angular-momentum vector, a constant couple acts on the latter and causes it to turn over and reverse its projection on H. The ion has then gained energy from the radiation field.

The resonance absorption can be detected by the loss of energy from the radiation field, which causes a lowering of the Q value of the cavity in which the paramagnetic substance is placed. The detecting system will be described in Section II. C.

Quantum mechanically, in the magnetic field H the levels corresponding to the various spatial orientations of J have energies

$$E = Mg\beta H, \tag{2.2}$$

where M is the magnetic quantum number and β is the Bohr magneton. The selection rules for magnetic-dipole transitions allow $M = \pm 1$. Therefore, the frequency of the transitions between the levels of Eq. (2.2) is given by

$$h\nu = g\beta H. \tag{2.3}$$

Because β is equal to $eh/4\pi mc$, Eqs. (2.3) and (2.1) will give the same frequency.

An experimentally determined g factor can be obtained with the aid of Eq. (2.3) by measuring resonance frequency and the corresponding magnetic field. If the paramagnetic atom or ion free or isolated, this g factor should be expected to correspond to the Lande formula,

$$g = 1 + \frac{J(J+1) + S(S+1) - L(L+1)}{2J(J+1)} . \qquad (2.4)$$

In fact, the experimentally determined g factor deviates greatly from that calculated from Eq. (2.4) and varies with the orientation of H with respect to the crystal-field axis. This anisotropy results from a combined effect of spin-orbit coupling and an incomplete "quenching" of the orbital angular momentum by the crystalline electric field. Thus each type of ion in a certain salt will give its own spectrum and therefore its own g value separated from those of other type ions. By comparing the observed g value with the calculated g value based on a certain electronic configuration and crystalline-field interaction we can obtain knowledge of the energy states of the ion.

B. Nuclear Interactions and Hyperfine Structure

When the nucleus of the paramagnetic ion also possesses a resultant angular momentum I, and hence a nuclear magnetic moment, (2I+1) different orientations of the nucleus in an external magnetic field thus produce (2I+1) component levels in each electronic state. A hyperfine structure is observed in the resonance spectrum. The splitting between the hyperfine lines is equal and independent of the external field, to a first approximation. The axis of quantization for the nucleus is provided by the very large field produced by the unpaired electrons (about 10^5 gauss), and hence the nuclei do not change their orientation during an electronic transition. In other words, the selection rule for the allowed transition is $\Delta m_I = 0$. If the nucleus has a quadrupole moment that interacts with the electric field gradient at the nucleus, a perturbation of the hyperfine-line energy levels results.

The spacings between hyperfine lines are no longer equal. In addition, the selection rule $\Delta M_I = 0$ is altered. Now $\Delta M_I = \pm 1$ and $\Delta M_I = \pm 2$ transitions become allowed, although they are not as probable as the $\Delta M_I = 0$ transitions.

From the hyperfine structure of the paramagnetic resonance, we can determine the nuclear spin and in some cases also the nuclear quadrupole moment of the ion studied. Conversely, when the nuclear spin of an ion is known, the hyperfine structure can be an identification of the ion studied. Protactinium-231 has a nuclear spin 3/2; four hyperfine lines are then expected in the resonance spectra.

C. Experimental Aspects

The general technique of measurements at centimeter wavelengths is applicable to paramagnetic resonance except that the sample is placed in a resonant cavity rather than in an extended wave guide. In this way, the sample may be located in a strong homogeneous magnetic field and the microwave field may be concentrated on the sample. The detecting system (the spectrometer) used in this work can be best illustrated by a block diagram (Fig. 1).

Microwave power from the Klystron (x-13 type) is transmitted through a gyrator and then through an attenuator to the E arm of a "magic tee." The frequency is measured by a frequency meter and regulated by an automatic frequency control. The H arm of the magic tee contains a crystal detector by means of which the signal is detected. One of the main arms contains slide screws and a matched load. Before resonance absorption, the screw is adjusted to balance the two arms of the bridge so that the signal delivered to the crystal is at a minimum. When the magnetic field is swept through a resonance point, microwave energy is absorbed by the sample in the cavity. This causes a lowering of the cavity Q and thus unbalances the bridge. A signal is then detected by the crystal in the H arm.

The magnetic field is modulated at 152 cps by coils wound on the periphery of the magnet pole pieces. Thus the signal delivered is proportional to the slope of the absorption peak.

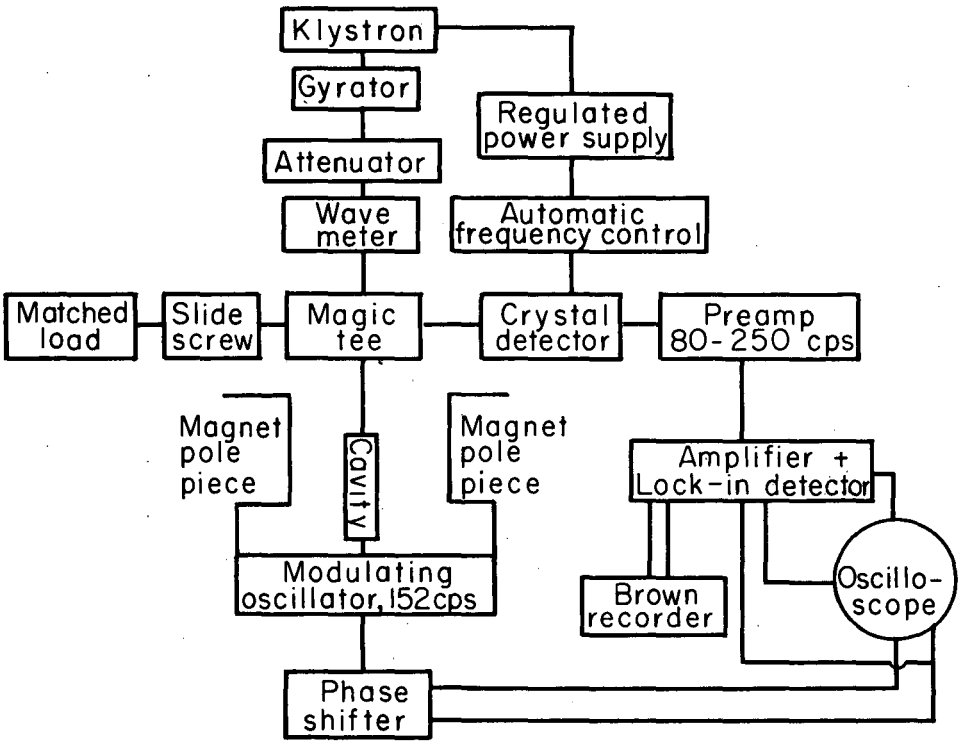

MU-19708

Fig. 1. Block diagram of the spectrometer.

The signal is delivered through a preamplifier and fed into the amplifier and phase-sensitive lock-in detector (80 to 250 cps) where it is converted into a dc signal which is displayed on an oscilloscope or recorded by a Brown recorder. The result on the Brown recorder chart is the derivative of an absorption.

One of the main factors governing the observation of paramagnetic-resonance absorption is the question of line width. Very wide lines are difficult to detect. A consideration of the various factors influencing the line width is helpful in the choice of a condition to reduce the line width.

(i) Spin-Lattice Relaxation

The absorption line broadening is produced by the interaction of the paramagnetic ions with the thermal vibrations of the lattice, a "smearing out" of their energy levels being thus produced. The "relaxation time," τ, is a measure of the time taken for the interaction to restore thermal equilibrium. The broadening produced by this interaction is given by[6]

$$\Delta\nu \approx \frac{1}{\tau} \propto T,$$

where $\Delta\nu$ is the broadening of the resonance frequency, τ is the relaxation time, and T is the absolute temperature. Therefore, in practice measurements are always made at lower temperatures--even down to $1^{\circ}K$--to reduce this kind of broadening. In the present work the paramagnetic resonance of Pa^{+4} was measured at the boiling point of liquid helium. In general, relaxation times longer than 10^{-7} sec give negligible contribution to line width compared with that from spin-spin interaction. If τ is longer than 10^{-5} sec, however, undesirable saturation effects appear, because the mechanism for transferring heat from the spin system to the lattice is unable to cope with the heat absorbed by the spin system from the radiation field. In consequence, the temperature of the spin system rises, and the intensity of the spectrum falls.

(ii) The Spin-Spin Interaction

This interaction is the mutual effect of one paramagnetic ion on another. Van Vleck derived an expression for the mean-square width of a line due to dipole-dipole interaction between free spins:[7]

$$(\Delta H)^2 = \frac{3}{4} S(S+1)\, g^2\beta^2 \sum_k \left\{ \frac{1-3\cos^2\theta}{r^3} \right\}_{jk}$$

$$+ \frac{1}{3} S'(S'+1) \frac{g'^4}{g^2} \beta^2 \sum \left\{ \frac{1-3\cos^2\theta}{r^3} \right\}^2_{jk} ,$$

where S and S' are the spins of the paramagnetic ions, g and g' are the spectroscopic splitting factors, and r is the distance apart of the j and kth ion, and θ is the angle between the r vector and the molecular axis. To a first order, spin-spin interaction is independent of the magnetic field strength and the temperature. Broadening by this effect may be reduced by moving the paramagnetic ions farther apart by diluting the salt with an isomorphous diamagnetic equivalent compound. In this work, Cs_2ZrCl_6 has been used as the diamagnetic diluent.

(iii) Exchange Interaction

The exchange interaction narrows the lines at the center and broadens them near the ends, leaving $(\Delta H)^2_{av}$ unchanged. But if the exchange is taking place between dissimilar ions, the exchange interaction will tend to bring two different transitions together and thus produce one wider line.

(iv) Inhomogeneous Fields

Line widths of under 0.1 gauss have been observed in highly homogeneous fields. For such observations, field homogeneity to one part in 10^5 may be required. This can be achieved by grinding and polishing the pole faces to optical flats. If the pole faces are not very large, careful shimming of the edges may be required in addition. Line broadening due to field inhomogenieties is not an intrinsic effect of the paramagnetic ions, of course.

III. THEORY OF PARAMAGNETIC RESONANCE[8]

A. Hamiltonian of an Ion in a Single Crystal and in the Presence of an External Magnetic Field

The general Hamiltonian can be described as consisting of eight terms:

$$W = W_1 + W_2 + W_3 + W_4 + W_5 + W_6 + W_7 + W_8 \tag{3.1}$$

The first term,[9]

$$W_1 = \sum_k \frac{P_k^2}{2m} - \frac{Ze^2}{r_k} + \sum_{j<k} \frac{e^2}{r_{jk}}, \tag{3.2}$$

is the coulomb interaction of the electrons with the nucleus and with each other. This interaction depends only on the electronic spatial configuration and causes a splitting of the energies of the various electron configurations of the ion of the order of 10^5 cm^{-1}. In paramagnetic resonance only the lowest energy levels are of importance, the higher levels associated with W_1 having no effect except when the ground state is not degenerate and the admixture of higher eigenstates of W_F is necessary to obtain the spin degeneracy.

The second term is defined by

$$W_2 = \sum_j - e\, V\,(x_j y_j z_j), \tag{3.3}$$

where V (xyz) is the crystalline field potential due mainly to the surrounding ions and dipoles. It causes a lifting of the degenercy of the ground state of W_1. The order of magnitude of this effect, the nature of the resulting energy levels, and the amount of degenercy remaining in them depends upon the symmetry of the crystal field and the nature of the wave function of the unpaired electrons. For instance, d orbitals suffer stronger crystalline-field splitting than the f functions. In the present case, in order to decide whether the Pa^{+4} possesses a 6d electron or a 5f electron, the splittings of the

energy levels of both the 6d and 5f configurations in the cubic crystalline field are studied in Sections (3.C) and (3.D).

The third term,

$$W_3 = \lambda \vec{L}.\vec{S}, \tag{3.4}$$

is the spin-orbit interaction term and is of the order of 10^2 cm^{-1}. Here λ is the spin-orbital coupling constant, L is the total angular momentum vector, and S is the total spin vector.

$$\mathbf{W}_4 = -\zeta \left[(\vec{L}.\vec{S})^2 + \frac{1}{2} (\vec{L}.\vec{S}) - \frac{1}{3} L(L+1) S(S+1) \right]$$

$$= -\zeta \left[\frac{1}{2} (L_i L_j + L_j L_i) S_i S_j - \frac{1}{3} L(L+1) S(S+1) \right], \tag{3.5}$$

where ζ is a constant coefficient for this term. This term represents the magnetic interaction between the spins and is of the order of magnitude of 1 cm^{-1}.

The fifth term,

$$W_5 = \Sigma \frac{eh}{4\pi mc} (\vec{L} + 2\vec{S})_k \cdot \vec{H} = \beta (\vec{L} + 2\vec{S}) \cdot \vec{H}, \tag{3.6}$$

is the effect of the external magnetic field. It produces the splitting of the electronic levels between which the transitions are observed and is about 1 cm^{-1}.

For the sixth term, we have

$$W_6 = \left(\frac{\bar{I}}{r^3}\right) 2\gamma\beta\beta_N \left[\vec{L}.\vec{I} + \xi \{\vec{L}(\vec{L}+1) (\vec{S}.\vec{I}) - \frac{3}{2} (\vec{L}.\vec{S}) (\vec{L}.\vec{I}) \right.$$

$$\left. - \frac{3}{2} (\vec{L}.\vec{I}) (\vec{L}.\vec{S}) \} - k\vec{S}.\vec{I} \right], \tag{3.7}$$

where β_N is the nuclear magneton, I is the nuclear-spin vector operator, and

$$\xi = \frac{2\ell+1 - 4S}{S(2\ell-1)(2\ell+3)(2\ell+1)} \tag{3.8}$$

is the interaction between the magnetic moment of the nucleus and the magnetic field set up by the orbital and spin moments of the electrons. This interaction is the cause of the hyperfine structure and is of the order of magnitude $\sim 10^{-2}$ cm^{-1}.

The seventh term is

$$W_7 = \frac{\eta e^2 q}{2I(2I-1)\, r^3} \left[3(\vec{L}.\vec{I})^2 + \frac{3}{2} (\vec{L}.\vec{I}) - L(L+1)\, I(I+1) \right], \tag{3.9}$$

which represents the nuclear-quadrupole interaction where q is the nuclear quadrupole interaction constant and

$$\eta = \pm 2S\xi \tag{3.10}$$

for $\ell = 2$. The sign of η depends on whether the shell is less than or more than half full.

The eighth term,

$$W_8 = -\gamma \cdot \beta_N \cdot H \cdot I,$$

is the direct effect of the applied magnetic field on the nuclear magnetic moment and is of the order of 10^{-3} cm^{-1}.

The ground term of the free ion is given by Hund's rule, and the result of various transformations of the different perturbations gives the first-order perturbation Hamiltonian:

$$\begin{aligned} W_0 = {} & V + (\lambda - \tfrac{1}{2}\zeta)(\vec{L}.\vec{S}) - \zeta (\vec{L}.\vec{S})^2 + \beta H.(\vec{L} + 2\vec{S}) + P[(\vec{L}.\vec{I}) \\ & + \{\xi\, L(L+1) - K\}(\vec{S}.\vec{I}) - \tfrac{3}{2}\xi (\vec{L}.\vec{S})(\vec{L}.\vec{I}) - \tfrac{3}{2}\xi (\vec{L}.\vec{I})(\vec{L}.\vec{S})] \\ & + q\{(\vec{L}.\vec{I}) + \tfrac{1}{2}(\vec{L}.\vec{I})\} - \gamma\beta_N (\vec{H}.\vec{I}) \end{aligned} \tag{3.12}$$

$$P = 2V\beta\beta_N / r^3 , \tag{3.13}$$

$$q = \eta e^2 Q/2I(2I-1)\, r^3 , \tag{3.14}$$

γ is the nuclear gyromagnetic ratio and Q is the nuclear quadrupole moment,

$$Q = \frac{i}{e} \int \rho_I \, (3Z^2 - \gamma^3)\, d\nu . \tag{3.15}$$

Here ρ_Z is the nuclear charge density, λ and ζ are constants for the particular ion, and ξ, η, and k are constants depending on the electronic configuration.

The separation between energy levels of V and the first-order spin-orbit coupling is much greater than the magnitude of the other terms in W_0. In order to study the energy levels of the paramagnetic ion under the influence of all these terms, the problem is usually treated in stages. The energy levels are first studied under the influence of crystalline electrostatic fields only, and then, with this as the unperturbed system, the spin-orbit coupling and the external magnetic field are treated as perturbations.

B. Derivation of the Spin Hamiltonian

Paramagnetic-resonance absorption occurs in the centimeter wave-length range. Only the lowest level of V enters into consideration, since the other levels are $\sim 10^4$ cm^{-1} above the lowest one. If the lowest level of V is nondegenerate orbitally, the contribution of the spin-orbit coupling vanishes in first order. If the lowest level of V possesses orbital degeneracy, then the first-order spin-orbit coupling will split this level into several Kramer's doublets. In both cases the degeneracy left in the lowest level is that arising from the electronic and nuclear spins. The first-order contribution from the remaining terms to the energy is then given by replacing all orbital variables in Eq. (3.12) by their expectation values. The expectation value of L is zero, that is,

$$<0|L_x|0> = <0|L_y|0> = <0|L_z|0> = 0 \tag{3.16}$$

where $<0|$ is the ground level. It follows then that

$$<0|0> = 1 \tag{3.17}$$

and

$$\frac{1}{2} <0|L_i L_j + L_j L_i|0> \equiv \frac{1}{3} L(L+1)\delta_{ij} + \ell_{ij}, \tag{3.18}$$

with

$$\ell_{ii} = 0. \tag{3.19}$$

Pryce has carried out perturbation calculations in which the operators referring to spin and nuclear variables are treated as noncommuting algebraic quantities.[10] That is, no representation is chosen for either S or I. The result of this is an expression that involves the components of S and I. The first-order terms are:

$$-\zeta \ell_{ij} S_i S_j + 2\beta H.S - \Gamma(k\delta_{ij} + 3\xi \ell_{ij}) S_i I_j$$

$$+ q' \ell_{ij} I_i I_j - \gamma \beta_N H.I, \tag{3.20}$$

where the indices ij refer to Cartesian coordinations and Γ is a constant.

The second-order contributions arising from the spin-orbit interaction and its joint effect with other terms usually cannot be neglected. They give rise to terms which must be added to Eq. (3.20). These second-order terms are:

$$-\lambda\{\lambda\Lambda_{ij} + \zeta(\mu_{ij} + \mu_{ji})\} S_i S_j - 2\lambda\beta\Lambda_{ij} H_i S_j$$

$$-\lambda P(2\Lambda_{ij} - 3\xi\mu_{ij}) S_i I_j \tag{3.21}$$

$$\text{where } \Lambda_{ij} = \Lambda_{ji} = \sum_{n \neq 0} \frac{\langle 0 \mid L_i \mid n \rangle \langle n \mid L_j \mid 0 \rangle}{E_n - E_0} \tag{3.22}$$

$$\mu_{ij} = \frac{i}{2} \ell_{ik\ell} \sum_{n \neq 0} \frac{\langle 0 \mid L_\ell \mid n \rangle \langle n \mid L_j L_k + L_k L_j \mid 0 \rangle}{E_n - E_0} \tag{3.23}$$

and

$$\mu_{ii} = 0. \tag{3.24}$$

Here the summation is over the energy levels of V, and the index 0 refers to the lowest level. Thus we obtain the spin Hamiltonian,

$$\begin{aligned} \mathcal{H} = & \{ -\lambda^2 \Lambda_{ij} - \zeta \ell_{ij} S_i S_j - \lambda \zeta (\mu_{ij} + \mu_{ji}) \} S_i S_j \\ & + 2\beta (\delta_{ij} - \lambda \Lambda_{ij}) H_i S_j - P(k \delta_{ij} + 3\xi \ell_{ij} + 2\Lambda_{ij} \\ & - 3\xi \lambda \mu_{ij}) S_i I_j + q \ell_{ij} I_i I_j - \gamma \beta_N H \cdot I , \end{aligned} \tag{3.25}$$

which can be abbreviated

$$\mathcal{H} = D_{ij} S_i S_j + \beta g_{ij} H_i S_i + A_{ij} S_i I_j + Q_{ij} I_i I_j - \gamma \beta_N H \cdot I . \tag{3.26}$$

This can also be written in the form:

$$\mathcal{H} = S.D.S + \beta H.g.S + S.T.I + I.P.I - \gamma \beta_N H.I. \tag{3.27}$$

In the x, y, z coordinate system it can be resolved into components along three principal axes x, y, z:

$$\mathcal{H} = \beta (g_z H_z S_z + g_x H_x S_x + g_y H_y S_y) + D \{ S_z^2 - \frac{1}{3} S(S+1) \}$$

$$+ E(S_x^2 - S_y^2) + A_z S_z I_z + A_x S_x I_x + A_y S_y I_y$$

$$+ P\{I_z^2 - \frac{1}{3} I(I+1)\} + P'(I_x^2 - I_y^2) - g_N \beta_N H.I. \qquad (3.28).$$

When the lowest level of V is an orbital singlet, the spin-orbit coupling vanishes in first order. In Eq. (3.28), S is the actual spin of the free ion. When the lowest level of V is degenerate orbitally, the effect of first-order spin-orbit coupling gives several Kramer's doublets which are complicated mixtures of the spin and orbital wave functions of the free ion. In the Hamiltonian, S is only a fictitious spin of the system and is defined simply by equating 2S+1 to the number of electronic levels in the lowest group. The coefficients $g_x g_y g_z$, D, E, $A_x A_y A_z$, P, P' S, and I can be determined experimentally. If the crystal field has axial symmetry, we have:

$$g_z = g_{||}, \quad g_x = g_y = g_{\perp} \qquad (3.29)$$

$$A_z = A, \quad A_x = A_y = B \qquad (3.30)$$

$$E = P' = 0. \qquad (3.31)$$

If the symmetry is exactly cubic, as in the present case of $PaCl_6^{=}$, the magnetic ion is surrounded by a regular octahedron of negative charges, and we have

$$g_x = g_y = g_z = g, \qquad (3.32)$$

$$A_x = A_y = A_z = A, \qquad (3.33)$$

and

$$D = E = P = P' = 0. \qquad (3.34)$$

C. Ground State of a 5f' Electron Configuration in an Octahedral Crystalline Field

Assumptions about the effect of a crystalline field on various magnetic ions can be divided into three classes on the basis of comparison with the relative magnitude of the effects of spin-orbit coupling and Russell-Saunder's coupling:

$$\text{For Spin-orbit coupling } \vec{L} + \vec{S} = \vec{J} \tag{3.35}$$

$$\text{For Russell-Saunders coupling } \sum_i \ell_i = \vec{L} \tag{3.36}$$

In a predominatly octahedral crystalline field; the expression for the field potential V is given by

$$V = C + T \tag{3.37}$$

where C, the cubic part of the crystalline field potential, is much greater than T, the lower symmetrical part of the crystalline field potential.

(1) The effect of V is smaller than both (3.35) and (3.36) so that L and S are coupled to a resultant J which will precess about the direction of the electric field and will be split into components corresponding to M_J quantum numbers. The rare-earth elements belong to this class because of the shielding of the 4f electrons from the direct effect of the crystalline electric field.[11]

(2) The effect of C is stronger than (3.35) but less than (3.36). Then L and S are uncoupled and each precesses separately about the direction of the electric field. The resulting energy levels are defined by quantum numbers M_L and M_S. If the splittings between different M_L levels are very large ($\sim 10^{-4}$ cm^{-1}) only the lowest level is populated at ordinary temperatures. Then the effects of (T + 3.35) are treated as perturbations to this lowest state. This occurs in the iron-group transition elements where the unpaired electrons are more directly affected by the crystalline field.[12]

(3) The effect of C is not only greater than (3.35) but also greater than (3.36). This is due to covalent bonding and has been studied mainly in ionic complexes.[13]

For a 5f electron, the 5f wave function is not so well screened as the 4f wave function. The crystalline-field interaction, though not as great as to the 3d electrons, may be increased to the same order of magnitude as the spin-orbit coupling. The resulting energy levels thus depend upon the relative magnitude of spin-orbit coupling and crystalline-field splitting. In an octahedral crystalline potential, the 5f orbitals undergo the splitting:

$$f(7) \rightarrow \Gamma_2\,(1) + \Gamma_4\,(3) + \Gamma_5\,(3) \tag{3.38}$$

where Γ_2, Γ_4, and Γ_5 are the representations of the cubic double group. The numbers in the parentheses indicate degeneracies.

The energies can be obtained by solution of the secular equation.

The crystalline potential can be expanded in spherical harmonics:

$$V = \sum_{nm} A_n^m \, \gamma^n \, Y_n^m \, (\theta, \phi).$$

In the case of an f electron, it is necessary to consider both the fourth-and sixth-degree terms in the octahedral potential:

$$V_{oct.} = A_4^o \left\{ Y_4^o + \sqrt{\frac{5}{14}} \, (Y_4^4 + Y_4^{-4}) \right\} + A_6^o \left\{ Y_6^o - \frac{\sqrt{14}}{2} (Y_6^4 + Y_6^{-4}) \right\}, \tag{3.39}$$

where

$$Y_n^m \, (\theta, \phi) = (-1)^n \left(\frac{(2n+1)\,(n-|m|)!}{2(n+|m|)!} \right)^{1/2} \frac{1}{\sqrt{2\pi}} \; P_n^{|m|} (\cos\theta) \, e^{im\phi} \tag{3.40}$$

and

$$P_n^m \, (x) = \frac{(1-x^2)^{m/2}}{2^n n!} \; \frac{d^{n+m}}{dx^{n+m}} \; (x^2 - 1)^n \; . \tag{3.41}$$

Substituting Eqs. (3.40) and (3.41) into (3.39), we can change the form for the potential to Cartesian coordinates:

$$V = B_4^o \Sigma (35Z^4 - 30\gamma^2 Z^2 + 3\gamma^4) + B_4^4 \Sigma (x^4 - 6x^2y^2 + y^4)$$

$$+ B_6^o \Sigma(231Z^6 - 315\gamma^2 Z^4 + 105\gamma^4 Z^2 - 5\gamma^6)$$

$$+ B_6^4 \Sigma(10\gamma^2 x^4 + 10\gamma^2 y^4 + 20\gamma^2 x^2 y^2 - 33x^4y^2 - 33x^2y^4 - 11y^6 - 11x^6) \tag{3.42}$$

where $B_4^o = \frac{3}{16\sqrt{\pi}} A_4^o$, $B_4^4 = \frac{3}{8}\left(\frac{35}{2\pi}\right)^{1/2}\left(\frac{5}{14}\right)^{1/2} A_4^o = \frac{15}{8}\left(\frac{1}{4\pi}\right)^{1/2} A_4^o$,

$$B_6^o = \left(\frac{13}{4\pi}\right)^{1/2} \frac{1}{16} A_6^o, \text{ and } B_6^4 = \left(\frac{13}{4\pi}\right)^{1/2} \frac{21}{16} A_6^o . \tag{3.43}$$

The elements in the secular determinant are the integrals $\int \psi_m^* (ev) \psi_m \, dr$. These can be obtained easily by replacing the coordinates by equivalent operators.[14] For example, the set of functions $x^2 - y^2$, $3z^2 - \gamma^2$, xy, yz, zx is proportional to $L_x^2 - L_y^2$, $3L_z^2 - L(L+1)$, $1/2\,(L_xL_y + L_yL_x)$, $1/2\,(L_yL_z + L_zL_y)$, $1/2\,L_zL_x + L_x L_z)$, and

$$\Sigma(35z^4 - 30\gamma^2 z^2 + \gamma^4) \equiv \beta\gamma^{-4}\,[35L_z^4 - 30L(L+1)L_z^2 + 25L_z^2 - 6L(L+1)$$

$$+ 3L^2(L+1)^2] \tag{3.44}$$

$$\Sigma\, 231z^6 - 315\gamma^2 z^4 + 105\gamma^4 z^2 - 5\gamma^6 = -\gamma\gamma^{-6}\,[231L_z^6 - 315L(L+1)L_z^4$$

$$+ 735L_z^4 + 105L^2(L+1)^2$$

$$L_z^2 - 525L(L+1)L_z^2 + 294L_z^2 - 5L^3(L+1)^3 + 40L^2(L+1)^2 - 60L(L+1). \tag{3.45}$$

Once the matrix element of V_s^o is obtained, we can calculate the matrix element of V_s^k easily from the relations

$$< L\, m_\ell \mid V_s^o \mid \ell\, m_\ell > = \alpha\, C^\ell_{m\ell o} \tag{3.46}$$

and

$$< Lm_\ell + k \mid V_s^k \mid \ell, m_\ell > = \alpha\, C^\ell_{m\ell k}\ , \tag{3.47}$$

where α's are the same in Eqs. (3.46) and (3.47) and depend on L and ℓ only and $C^\ell_{m\ell o}$ and $C^\ell_{m\ell k}$ are Wigner coefficients. For $C^\ell_{m\ell m'}$, we have

$$C^\ell_{m\ell m'} = \sum_\nu \frac{(-1)^\nu [(\ell+m_\ell)!\,(\ell-m_\ell)!\,(S+m')!\,(S-m')!\,(\ell+M)!\,(\ell-M)!]^{1/2}}{(\ell-m_\ell-\nu)!\,(\ell+m_\ell-\lambda+\nu)!\,(S+m'-\nu)!\,(S-m'-\lambda+\nu)!\,\nu!\,(\lambda-\nu)!}\ , \tag{3.48}$$

where $m' = 0$ for $C^\ell_{m_\ell o}$, $m' = k$ for $C^\ell_{m_\ell k}$, $M = m_\ell + m'$, and $\lambda = \ell + S - L = S$ when $L = \ell$ as in the present case. The matrix elements only couple states in the same L manifolds.

Knowing $< L, m_\ell \mid V_s^o \mid L, m_\ell >$, α, $C^\ell_{m\ell o}$, and $C^\ell_{m\ell k}$, we can easily calculate $< L, m_\ell + k \mid V_s^k \mid L, m_\ell >$. In this way we obtain the following determinant of the secular equation for the splittings of the 5f orbitals as in Eq. (3.38):

$$\langle m_\ell \,|\, -e\, V_{oct} \,|\, m'_\ell \rangle$$

	3	2	1	0	-1	-2	-3
3	$3a' - b/7 - \lambda$				$\sqrt{15}a' + \sqrt{15}b'$		
2		$-7a' + 6/7\, b' - \lambda$				$5a' - 6b'$	
1			$a' - (15/7)b' - \lambda$				$\sqrt{15}a' + \sqrt{15}b'$
0				$6a' + 20b'/7 - \lambda$			
-1	$\sqrt{15}\, a' + \sqrt{15}b'$				$a' - 15b'/7 - \lambda$		
-2		$5a' - 6b'$				$-7a' + 6b'/7 - \lambda$	
-3			$\sqrt{15}a' + \sqrt{15}b'$				$3a' - b'/7 - \lambda$

where a' and b' are positive numbers:

$$a' = \frac{180}{16\sqrt{\pi}} A_4^o \beta r_e^4 \qquad b' = -\left(\frac{13}{4\pi}\right)^{1/2} \frac{1260}{16} A_6^o \gamma r_e^6 \tag{3.49}$$

The matrix for the secular equation can be factored:

$$\begin{array}{c|c} & |0> \\ \hline <0| & \boxed{6a' + \frac{20}{7} b' - \lambda} \end{array} \qquad \lambda_1 = 6a' + \frac{20}{7} b' \tag{3.50}$$

$$\begin{array}{c|cc} & |\pm 2> & |\mp 2> \\ \hline <\pm 2| & -7a' + \frac{6}{7} b' - \lambda & 5a' - 6b' \\ <\mp 2| & 5a' - 6b' & -7a' + \frac{6}{7} b' - \lambda \end{array}$$

$$(-7a' + \frac{6}{7} b' - \lambda)^2 - (5a' - 6b')^2 = 0$$

$$\lambda_2 = 2a' - \frac{36}{7} b' \tag{3.51}$$

$$\lambda_3 = 12a' + \frac{48}{7} b' \tag{3.52}$$

$$\begin{array}{c|cc} & |\pm 3> & |\mp 1> \\ \hline <\pm 3| & 3a' - \frac{b'}{7} - \lambda & \sqrt{15}a' + \sqrt{15}b' \\ <\mp 1| & \sqrt{15}a' + \sqrt{15}b' & a' - \frac{15}{7} b' - \lambda \end{array}$$

$$(3a' - \frac{b'}{7} - \lambda)(a' \frac{15}{7} b' - \lambda) - (\sqrt{15}a' + \sqrt{15}b')^2 = 0$$

$$\lambda_4 = \lambda_1 = 6a' + \frac{20}{7} b' \tag{3.53}$$

$$\lambda_5 = \lambda_2 = -2a' - \frac{36}{7} b' \tag{3.54}$$

$$E(\Gamma_4) = 6a' + \frac{20}{7} b'$$

$$E(\Gamma_5) = -2a' - \frac{36}{7} b'$$

$$E(\Gamma_2) = -12a' + \frac{48}{7}$$

Taking Γ_4 as the zero energy $[E(\Gamma_4) = 0]$, we have

$$E(\Gamma_5) = -8a' - \frac{56}{7} b' = -8(a'+b') \tag{3.55}$$

and

$$E(\Gamma_2) = -18a' + \frac{28}{7} b' = -18a' + 4b' . \tag{3.56}$$

The corresponding eigenstates are:

$$|\Gamma_2> = \frac{1}{\sqrt{2}} |2> - \sqrt{\frac{1}{2}} |\bar{2}>$$

$$|\Gamma_5^1> = \sqrt{\frac{3}{8}} |3> - \sqrt{\frac{5}{8}} |\bar{1}>$$

$$|\Gamma_5^2> = \sqrt{\frac{3}{8}} |\bar{3}> - \sqrt{\frac{5}{8}} |1>$$

$$|\Gamma_5^3> = \sqrt{\frac{1}{2}} |2> + \sqrt{\frac{1}{2}} |\bar{2}>$$

$$|\Gamma_4^1> = \sqrt{\frac{5}{8}} |3> + \sqrt{\frac{3}{8}} |1>$$

$$|\Gamma_4^2> = \sqrt{\frac{5}{8}} |\bar{3}> + \sqrt{\frac{3}{8}} |1>$$

$$|\Gamma_4^3> = |0>.$$

It is assumed[15] that Γ_4 orbitals are involved in the binding of the chlorine atoms to the protactinium and that, as a result, $E(\Gamma_4)$ is promoted to high values and will always be the highest of the three energies. However, $E(\Gamma_5) - E(\Gamma_2)$ may be either + or - depending upon the relative magnitude of a and b.

Let

$$\xi = \frac{E(\Gamma_4) - E(\Gamma_5)}{E(\Gamma_5) - E(\Gamma_2)} \tag{3.57}$$

Here ξ will be + or - depending upon $E(\Gamma_5) - E(\Gamma_2)$ being + or -.

The addition of spin gives the additional splittings:

$$\begin{aligned} \Gamma_2 &\rightarrow \Gamma_7\,(2) \\ \Gamma_4 &\rightarrow \Gamma_6^{(2)} + \Gamma'_8\,(4) \\ \Gamma_5 &\rightarrow \Gamma'_7\,(2) + \Gamma_8\,(4). \end{aligned} \tag{3.58}$$

Let $\alpha = \dfrac{\zeta}{E(\Gamma_5) - E(\Gamma_2)}$, where ζ is the spin-orbit coupling coupling constant. The energy of various energy states then depends upon the two parameters ξ and α. Solution of the quadratic equations provides energy eigenvalues and eigenfunctions for all values of ξ and α.

The energy curves versus α are shown in Fig. 2. In the left half of the figure, $E(\Gamma_5)$ is greater than $E(\Gamma_2)$, α is +, and ξ is +. In the right half $E(\Gamma_5)$ is less than $E(\Gamma_2)$, α is -, and ξ is -. On either side, a Γ_7 state is lowest. The number after each representation denotes the value of ξ which is given by Eq. (3.57) in the absence of spin-orbit coupling. The energy is given in units of $E(\Gamma_5) - E(\Gamma_2)$ in the extreme left fourth of the figure, and in units of $E(\Gamma_2) - E(\Gamma_5)$ in the extreme right fourth.

In the central one-half of the figure, the energy is given in units of ζ, the spin-orbit coupling constant. The Γ_7 and Γ'_7 energies are uninfluenced by the value of ξ. Since Γ_4 gives no Γ_7 state, when it is decomposed under spin-orbit coupling, the height

of $E(\Gamma_4)$ is of no consequence for $E(\Gamma_7)$ and $E(\Gamma'_7)$. The value of $E(\Gamma_7)$ or $E(\Gamma'_7)$ is taken as zero. These two states may be expressed in terms of basic states $M_\ell = 3, 2, 1, 0, \bar{1}, \bar{2}, \bar{3}$; $S_z = +, -$, from the matrix determinant given on the next page. Thus:

$$|\Gamma_{7+}> = \left\{\sqrt{\frac{1}{2}}\ A_n + \sqrt{\frac{1}{6}}\ B_n\right\} |2+> + \left\{-\sqrt{\frac{1}{2}}\ A_n + \sqrt{\frac{1}{6}}\ B_n\right\} |\bar{2}+> + B_n \left\{\frac{1}{2}|3->-\sqrt{\frac{5}{12}}\ |\bar{1}->\right\} \tag{3.59}$$

and

$$|\Gamma'_{7+}> = \left\{\sqrt{\frac{1}{6}}\ A_n - \sqrt{\frac{1}{2}}\ B_n\right\} |2+> + \left\{\sqrt{\frac{1}{6}}\ A_n + \sqrt{\frac{1}{2}}\ B_n\right\} |\bar{2}+> + A_n \left\{\frac{1}{2}|3->-\sqrt{\frac{5}{12}}\ |\bar{1}->\right\} \tag{3.60}$$

where $A_n = \dfrac{A}{\{A^2 + B^2\}^{1/2}}$, $B_n = \dfrac{B}{\{A^2 + B^2\}^{1/2}}$ (3.61)

$$A = 1 - \frac{a}{2} + \{1 - a + \frac{49}{4}\ a^2\}^{1/2} , \tag{3.62}$$

and

$$B = -2\sqrt{3}a . \tag{3.63}$$

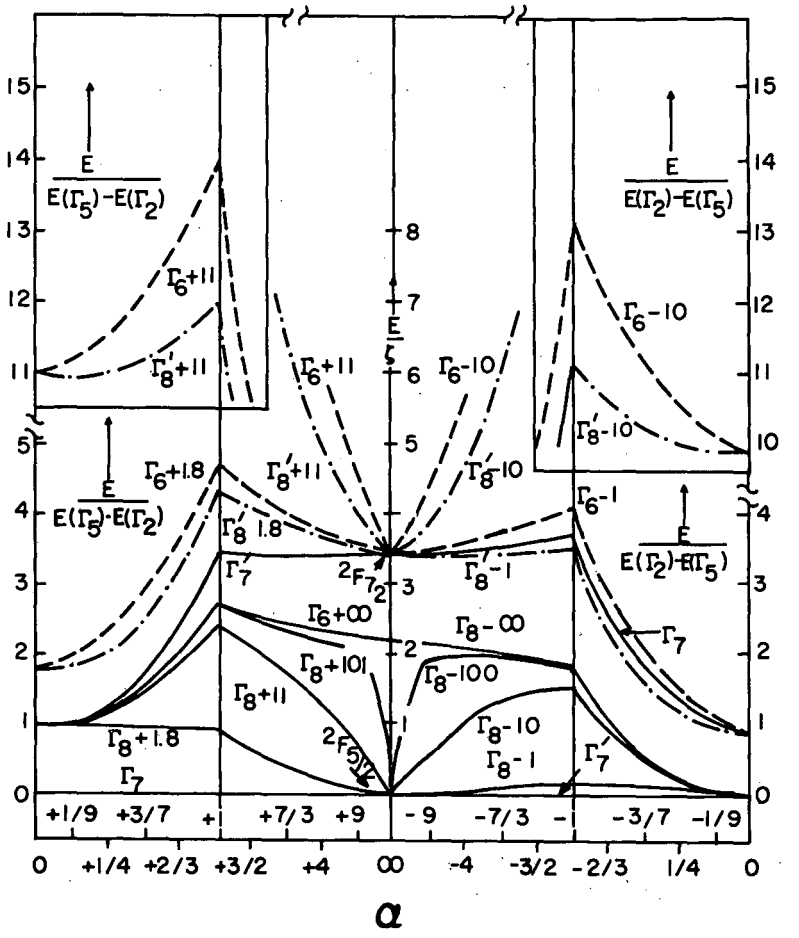

MU-19709

Fig. 2. Energy curves of a 5f' electron in an octahedral crystalline field.

$$\langle m_\ell\, S_Z \,|\, -eV_{oct} + \zeta\, L.S \,|\, m_\ell'\, S_Z \rangle$$

	$\|3+\rangle$	$\|3-\rangle$	$\|2+\rangle$	$\|2-\rangle$	$\|1+\rangle$	$\|1-\rangle$	$\|0+\rangle$
$\langle 3+\|$	$3a' - \frac{b'}{7} + \frac{3}{2}\zeta - \lambda$						
$\langle 3-\|$		$3a' - b'/7 - \frac{3}{2}\zeta - \lambda$	$\sqrt{\frac{6}{2}}\,\zeta$				
$\langle 2+\|$		$\sqrt{\frac{6}{2}}\,\zeta$	$-7a' + \frac{6}{7}b' + \zeta - \lambda$				
$\langle 2-\|$				$-7a' + \frac{6}{7}b'\,\zeta - \lambda$	$\frac{\sqrt{10}}{2}\,\zeta$		
$\langle 1+\|$				$\frac{\sqrt{10}}{2}\,\zeta$	$a' - \frac{15}{7}b' + \frac{1}{2}\zeta - \lambda$		
$\langle 1-\|$						$a' - \frac{15}{7}b' - \frac{\zeta}{2} - \lambda$	$\sqrt{3}\,\zeta$
$\langle 0+\|$						$\sqrt{3}\,\zeta$	$6a' + \frac{20b'}{7} - \lambda$
$\langle 0-\|$							
$\langle -1+\|$	$\sqrt{15}a' + \sqrt{15}b'$						
$\langle -1-\|$		$\sqrt{15}a' + \sqrt{15}b'$					
$\langle -2+\|$			$5a' - 6b'$				
$\langle -2-\|$				$5a' - 6b'$			
$\langle -3+\|$					$\sqrt{15}\,a' + \sqrt{15}\,b'$		
$\langle -3-\|$						$\sqrt{15}a' + \sqrt{15}\,b'$	

$\langle 3+\|$	$\|0-\rangle$	$\|-1+\rangle$	$\|\bar{1}-\rangle$	$\|\bar{2}+\rangle$	$\|\bar{2}-\rangle$	$\|\bar{3}+\rangle$	$\|\bar{3}-\rangle$
$\langle 3-\|$		$\sqrt{15}a' + \sqrt{15}b'$					
$\langle 2+\|$			$\sqrt{15}a' + \sqrt{15}b'$				
$\langle 2-\|$				$5a' - 6b'$			
$\langle 1+\|$					$5a' - 6b'$		
$\langle 1-\|$						$\sqrt{15}a' + \sqrt{15}b'$	
$\langle 0+\|$							$\sqrt{15}a' + \sqrt{15}b'$
$\langle 0-\|$							
$\langle -1+\|$	$6a' + \frac{20b'}{7} - \lambda$	$\sqrt{3}\zeta$					
$\langle -1-\|$	$\sqrt{3}\zeta$	$a' - \frac{15}{7}b' - \frac{\zeta}{2} - \lambda$					
$\langle -2+\|$			$a' - 15b' + \frac{\zeta}{2} - \lambda$	$\frac{\sqrt{10}}{2}\,\zeta$			
$\langle -2-\|$			$\frac{\sqrt{10}}{2}\,\zeta$	$-7a' + 6b' - \zeta - \lambda$			
$\langle -3+\|$					$-7a' + \frac{6}{7}b' + \zeta - \lambda$	$\frac{\sqrt{6}}{2}\,\zeta$	
$\langle -3-\|$					$\frac{\sqrt{6}}{2}\,\zeta$	$3a' - \frac{b'}{7} - \frac{3}{2}\zeta - \lambda$	
							$3a' - \frac{b'}{7} + \frac{3}{2}\zeta - \lambda$

From the Γ_7 state (i.e. when α is positive), we can obtain

$$g = 2 < \Gamma_7 \mid L_z + 2S_z \mid \Gamma_{7+} > = 2 \left\{ A_n^2 + 4\sqrt{\frac{1}{3}}\, A_n B_n \right\} . \tag{3.64}$$

From Γ'_A, we can obtain

$$g = 2 < \Gamma'_7 + \mid L_z + 2S_z \mid \Gamma'_{7+} > = 2 \left\{ B_n^2 - 4\sqrt{\frac{1}{3}}\, A_n B_n \right\} . \tag{3.65}$$

The variation of g with α is shown in Fig. 3. In the left half of the figure, $E(\Gamma_5) - E(\Gamma_2)$ is greater than zero and α is positive. In the right half of the figure, α is negative.

D. <u>Ground State of a 6d' Electron in the Octahedral Crystalline Field</u>.

The theory is similar to a 4d' or 5d' complex ion. The 6d wave function is extended far outwardly so that its interaction with the crystalline field is strong enough to break down not only the spin-orbit coupling, but also the ℓ-ℓ part of the Russell-Saunders coupling. The five d orbitals in an octahedral potential are split by the electric field into a lower level of $d\epsilon$ $\begin{matrix} xy \\ yz \\ zx \end{matrix}$ orbitals and an upper level of $d\gamma$ $\begin{matrix} x^2 - y^2 \\ 2z^2 - \gamma^2 \end{matrix}$ orbitals because the associated charge clouds avoid the attached negative charges from the chlorine ion (Fig. 4).

The formation of σ bonds with the chlorine atoms will further increase the splitting between the $d\epsilon$ triplet and the $d\gamma$ doublet, so that effectively two subshells are formed. The d electrons do not then give the usual L-S terms. They all go into the lower subshell dxy dyz dzx and form terms of which the one with the highest multiplicity consistent with Pauli's principle lies lowest (cf. Hund's rule). The lowest term for $(d\epsilon)'$ can be simply represented as having total spin $S = 1/2$ and total effective orbital angular momentum $L' = 1$:

$$(2L' + 1)(2S + 1) = 6.$$

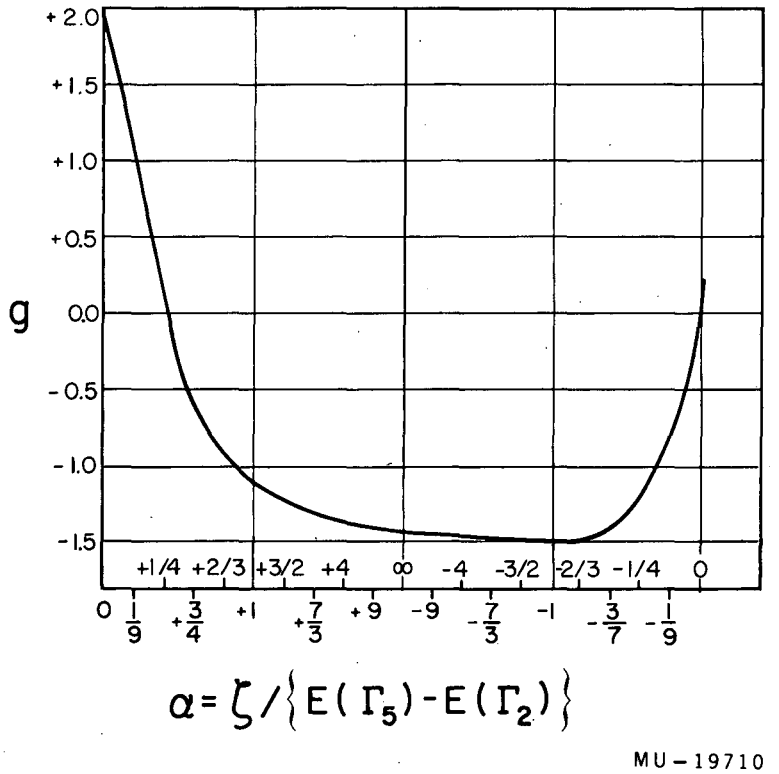

Fig. 3. Variation of g with α.

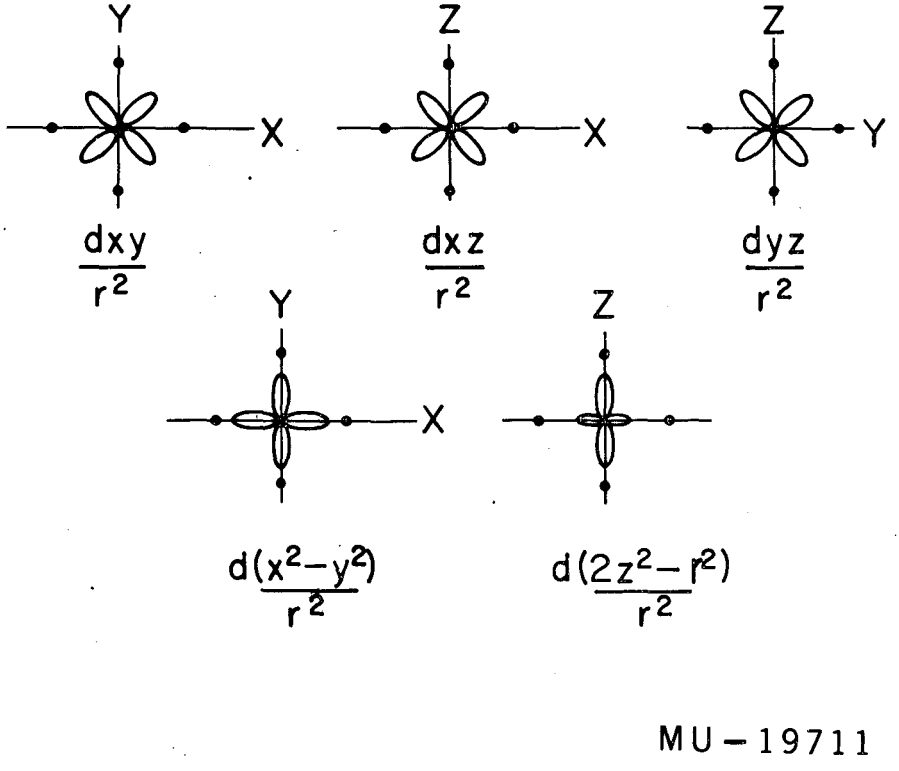

Fig. 4. Diagrams of the charge clouds associated with the orbitals of a d electron on a paramagnetic ion. The dots on the axes represent the negative ions (or molecules) of the octahedral complex as Cl^- ion in $PaCl_6^{=}$.

Therefore the level $(d\epsilon)'$ is sixfold degenerate. Spin-orbit interaction splits this into two levels: doublet at $+\zeta$, and quadruplet at $-1/2\zeta$ (Fig. 5a), where ζ is the spin-orbit coupling coefficient for a 6d electron. It has the order of magnitude of several thousand cm^{-1}. In paramagnetic resonance, normally only the transitions between the lowest (most highly populated) levels can be observed. Kotani has shown that the lowest quadruplet can be further split into two doublets by the magnetic field and has calculated the energy of the doublets up to the second order of magnetic field intensity:[16]

$$-1/2\ \zeta \text{ (doubly degenerate)}$$

$$-1/2\ \zeta - 4/3\ \beta^2/\zeta\ H^2 \text{ (doubly degenerate)}.$$

Therefore, in the energy range of paramagnetic resonance, no absorption can be seen unless the octahedral field is distorted to some lower symmetry. In fact, in all cases where there is orbital degeneracy, it is reasonable to expect that some distortion of the octahedral complex may occur to remove the orbital degeneracy in accordance with the theorem of John and Teller.[17] In addition, other ions besides chlorine in the crystal may set up a crystal field of low symmetry. If there is trigonal or tetragonal distortion, the lowest triplet is split into a spin doublet at $-2/3\,\Delta$ and two spin doublets at $+1/3\,\Delta$. The spin-orbit coupling leaves three Kramer's doublets (Fig. 5b) at[18]

$$\frac{1}{2}\left[\left(\frac{1}{2}\zeta - \frac{1}{3}\Delta\right) \pm \sqrt{\left(\frac{9}{4}\zeta^2 + \Delta\zeta + \Delta^2\right)}\ \right]\left(+\frac{1}{3}\Delta - \frac{1}{2}\zeta\right)$$

where ζ is positive, we assume that Δ is positive and the ground doublet of $(d\epsilon)'$ is at $\frac{1}{2}\left[\left(\frac{1}{2}\zeta - \frac{1}{3}\Delta\right) - \sqrt{\frac{9}{4}\zeta^2 + \Delta\zeta + \Delta^2}\right]$. When Δ is zero, this coincides with another doublet and as Δ goes negative, the ground level is at $(\frac{1}{3}\Delta - \frac{1}{2}\zeta)$. The spectroscopic splitting factors of the lowest doublet are therefore anisotropic.

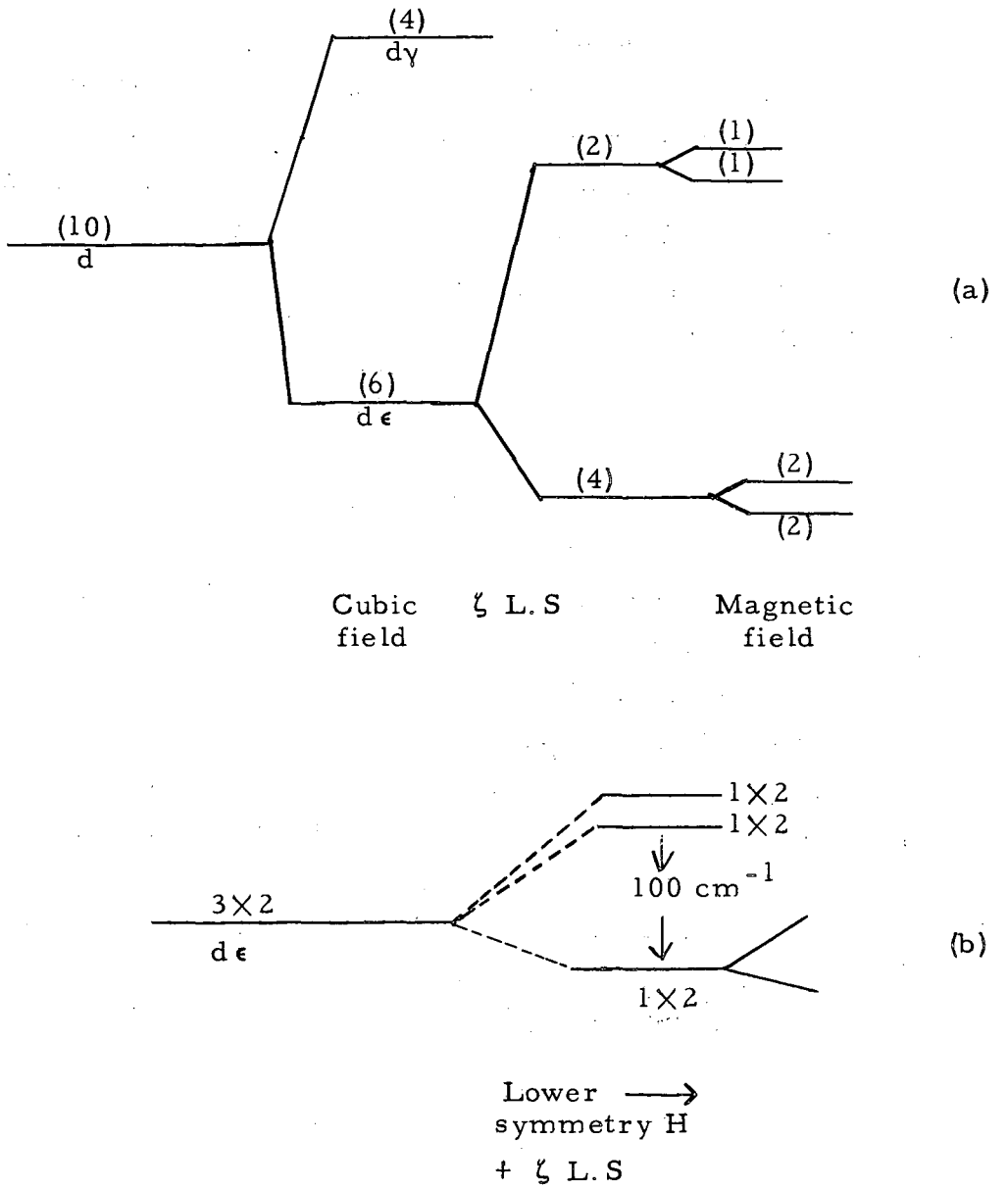

Fig. 5. Splitting of d' energy levels in octahedral complexes on a strong crystal-field model (a) without distortion of the complex according to Kotani[16] and (b) with distortion of the complex by lower symmetry.

Griffiths, Owen, and Ward give the following equations:[19]

With Δ + Ve: $g_{||} = -1 + 3\,(\Delta + \frac{1}{2}\zeta)/S$

$$g_{\perp} = 1 + (\Delta - \frac{3}{2}\zeta)/S\,,$$

where $S' = [\,(\Delta + \frac{1}{2}\zeta)^2 + 2\zeta^2\,]^{1/2}$;

With Δ - Ve: $g_{||} = g_{\perp} = 0$,

because the lowest level has no first-order Zeeman effect.[20] The change of the g value with the parameter Δ/ζ is shown in Fig. 6.

IV. EXPERIMENTAL PROCEDURE

A. Isolation of Pa^{+5} in Solution from Cationic Impurities.

The original solution from Harwell contained 8 mg of Pa^{231} in 33 ml of 6 M HCl + 0.5 M HF. Spectroanalysis showed the presence of a number of impurities (Table I).

Table I

Catonic impurities in solutions of Pa^{231}

Cation	Percent by weight	
	Before purification	After purification
Al	25	0.5
Ca	25	0.2
Nb	15	<0.01
Fe	2.5	0.25
Mg	2.5	0.05
Mn	0.5	<0.01
Pb	0.5	<0.01

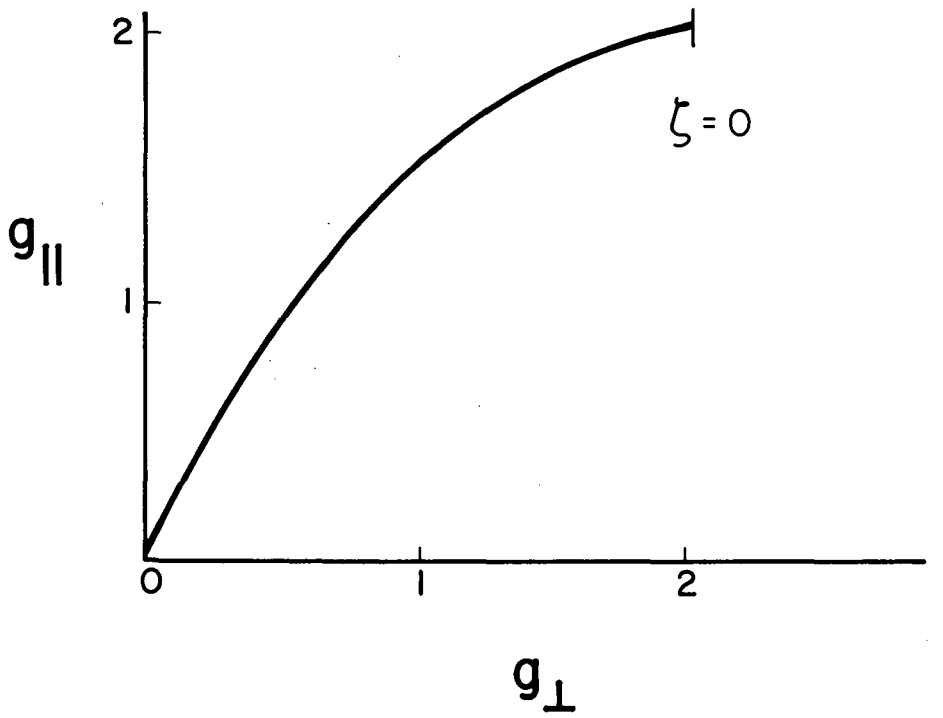

MU-19712

Fig. 6. Variation of the spectroscopic factors with the parameter Δ/ζ .

Twenty to thirty percent of the total alpha activity was found to be due to the decay daughters.

These impurities were removed by ion-exchange method of Kraus and Moore using Dowex A-1 anion exchange resin.[21] They studied the distribution of protactinium between hydrochloric acid solutions of different concentrations and the anion-exchange resin Dowex A-1 and showed that at 8 M and higher concentrations of hydrochloric acid, protactinium is absorbed by the resin. The adsorbed protactinium can then be washed with a large volume of 8 M or higher hydrochloric acid without eluting the protactinium. But the addition of a very small amount of HF to the HCl eluant causes protactinium to be rapidly desorbed from the column. Kraus and Moore utilized this characteristic to separate protactinium from niobium and tantalum, since these elements are eluted much more slowly by the HCl-HF eluant than is protactinium.[22] The same authors have similarly separated protactinium and iron.[23] Both protactinium and iron (III) are adsorbed on a column of Dowex A-1 resin from 9 M hydrochloric acid solution. The protactinium is then eluted with 9.0 M HCl--0.1 M HF, leaving iron (III) on the column. Aluminium and other ions that are not adsorbed by the resin at 9 M HCl can be separated by eluting first with 9 M HCl. The adsorbed protactinium can then be eluted with 9 M HCl--0.04 M HF.

The ion-exchange column was built from a polystyrene plastic tube of 6 mm diameter and polyethylene washing-bottle tip to avoid the reaction of HF with glass and adsorption of protactinium on the glass walls. Teflon shavings were used in place of glass wool at the tip of the column. The 200 to 400 mesh Dowex A-1 anion-exchange resin, previously washed with conductivity water and the 9 M HCl, was packed to a height of 9 cm. The flow rate was about 0.6 $ml/cm^2/min$.

The original solution containing 0.5 N HF was first evaporated to dryness to get rid of the hydrofluoric acid. The residue was dissolved in 1 ml of 9 M HCl, redissolved in 1 ml 9 M HCl, and then added to the top of the resin, followed by a few millimeters of

additional resin previously washed with 9 M HCl. The dilution was carried out with 5 ml of 9 M HCl first, then with ~8 ml of 9 M HCl--0.04 M HF mixture until all the protactinium activity came out of the column, as checked by an α meter. One hundred micrograms of the purified Pa were taken out for spectronanalysis. The result, given in Table I showed that the impurities were greatly reduced. Spectroanalysis of a blank HCl-HF mixture showed that all impurities present in the final product were present in equal or greater concentration of HCl-HF eluant.

A band of alpha activity was associated with the Pa^{231} band. In addition, another band of alpha activity was found in the 9 M HCl effluent. About 74% of the total activity was in the HCl-HF effluent; the remaining activity was in the 9 M HCl peak, as shown in Fig. 7.

As the activity of the original solution contained 20 to 30% of daughter activity, plates were made of the activities at the two peaks for pulse analysis. The result (Fig. 8) shows that the other peak is due to Pa^{231} daughter activities. Figure 9 shows the decay series of Pa^{231} from the Table of Isotopes.[24] From a comparison of the alpha-particle energies found for the peaks in Fig. 7, it is determined that the pulse-analysis peaks are due to Ra, Th, Bi, Rn, and Po, while the HCl-HF effluent peak is due only to Pa^{231} (Fig. 10). Thus the purified protactinium is also free from contamination of its alpha-active decay daughters.

B. Preparation of Solid $PaCl_4$

The existence of a tetravalent state of protactinium has been demonstrated by the preparation and identification of the dioxide, tetrachloride, and tetrafluoride by several workers[25] among them Elson, Fried, Sellers, and Zachariasen.[26] These authors obtained solid $PaCl_4$ by reactions in vacuum. Their methods were adopted because of the sublimation properties of $PaCl_4$ and $PaCl_5$, which facilitates the separation of the products from the residue materials. On the other hand, protactinium in aqueous solutions possesses a complex behavior.

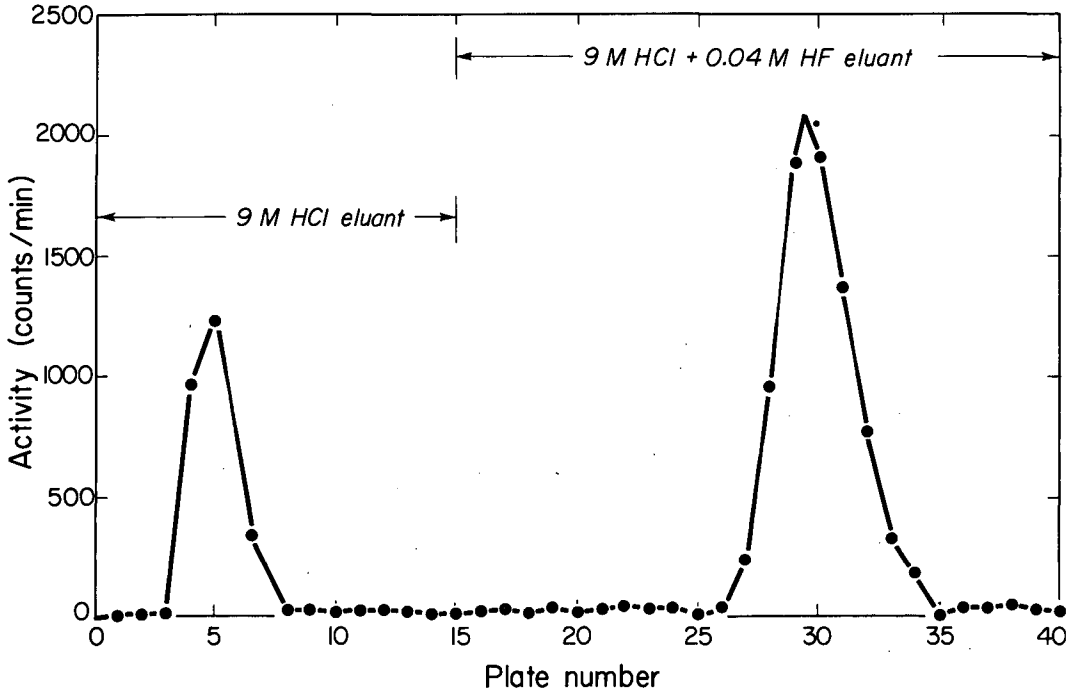

MU-18286

Fig. 7. Separation of activity on Dowex A-1 anion-exchange resin.

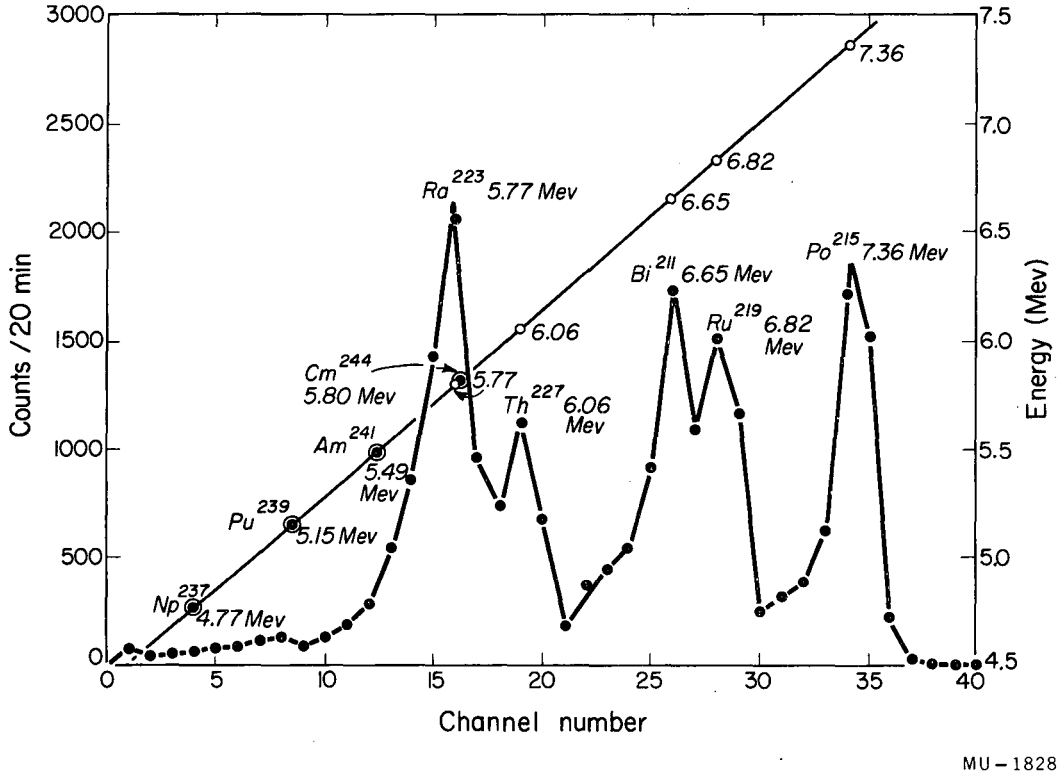

Fig. 8. Pulse analysis of plate No. 5, with amplifier setting of 885-8-550. The straight line corresponds to the correct scale for energy calibration of different channels by use of known energies of Np^{237}, Pu^{239}, Am^{241}, and Cm^{244}.

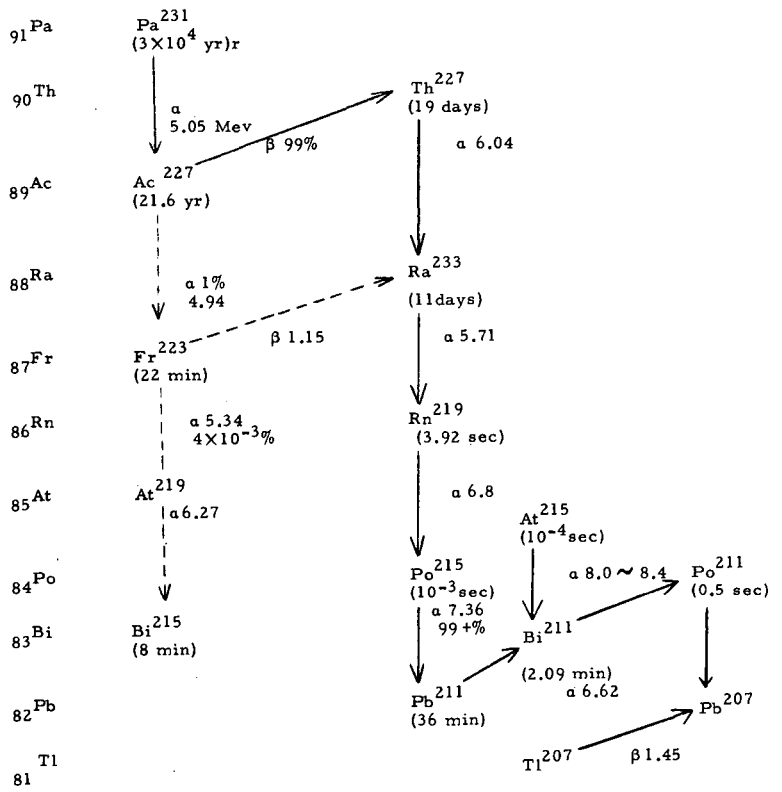

MU-19659

Fig. 9. Decay Series of Pa^{231}
Solid lines: major chain 99%
Dashed lines: minor chain 1%

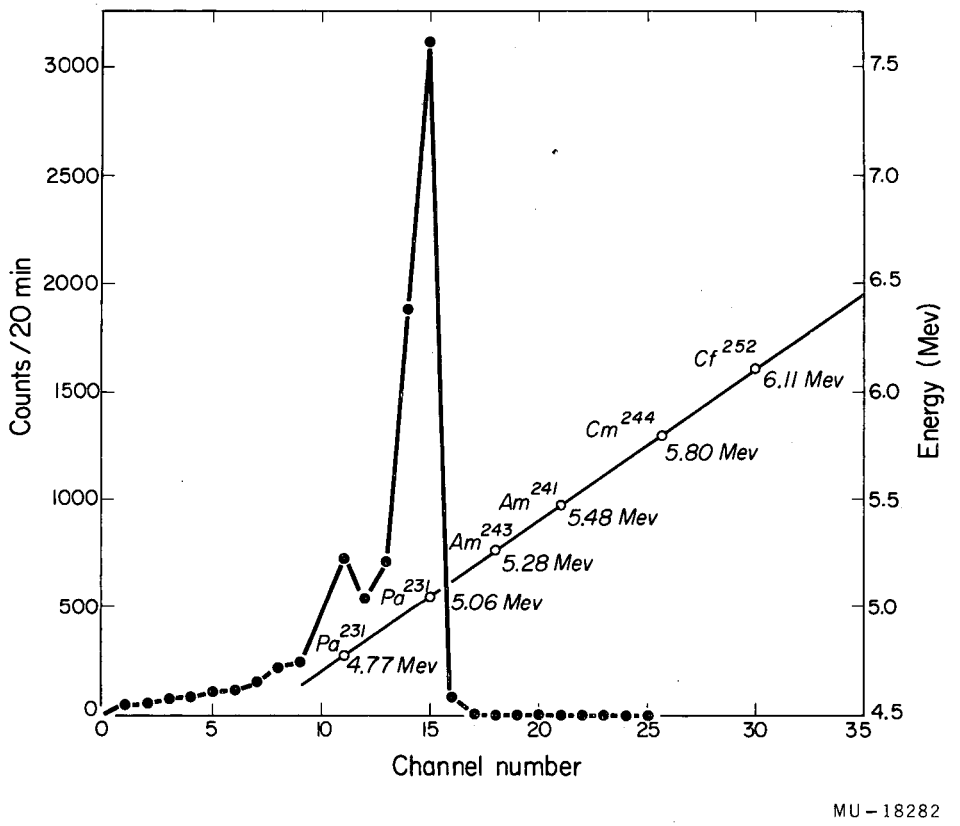

Fig. 10. Pulse analysis of plate No. 30 from the second peak, with amplifier setting of 385-9-510. The straight line is for energy calibration of the different channels. Palladium-231 has different modes of α decay and, thus, different α-particle energies from 5.05 to 4.66. The small peak is thought to be due to another mode of decay.

The method consists of three steps:

(a) Pa^{+5} in solution $\xrightarrow[NH_4OH]{ppt}$ $Pa(OH)_5$ (white) (dried at 70°).

(b) dry hydroxide (or hydrated oxide) $\xrightarrow[400\text{-}420^o]{CCl_4}$ $PaCl_5$ in vacuum (white)

(c) $PaCl_5 \xrightarrow[800^o]{H_2\ 150\ mm}$ $PaCl_4$ (greenish yellow).

Approximately 400 μg of the purified protactinium were precipitated with 12 M NH_4OH prepared by bubbling NH_3 gas into pure conductivity water. The precipitate [$Pa(OH)_5$] was collected by centrifugation in microcentrifuge cone and the supernatant discarded. After being washed three times, it was oven-dried overnight at 70^oC. The dried hydroxide shank from the wall of the centrifuge cone and could be easily transferred to a 20-cm-long quartz capillary drawn from a 14/35 quartz standard taper. The capillary, connected to the vacuum system, served as the container in which the reactions took place (chlorination and reduction), as well as for x-ray diffraction study of the crystal structure of the product.

The assembly of the reaction system is shown in Fig. 11. Tubes 1 and 2 are containers for carbon tetrachloride which was purified from dissolved gas by evaporation and condensation several times. Tube 3, which is surrounded by a furnace, contains UH_3 whose thermal decomposition produces hydrogen gas. In order to obtain 150 mm pressure of H_2 gas, the furnace was heated to 350^oC. The decomposed UH_3 can be recovered by filling the tube with tank hydrogen gas.

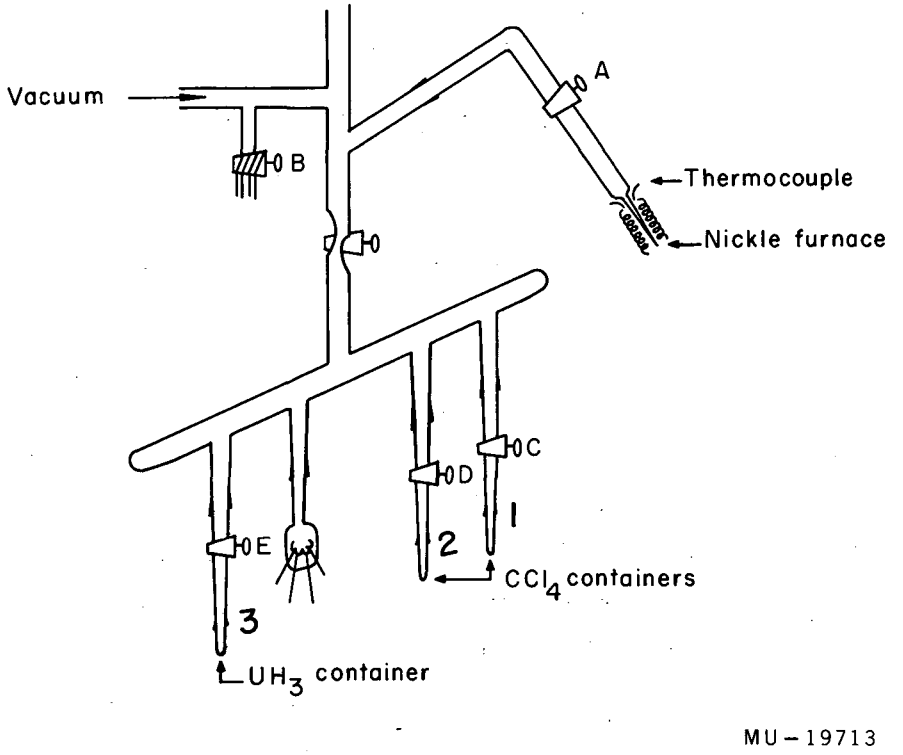

Fig. 11. Assembly for the preparation of $PaCl_5$ and $PaCl_4$.

By manipulation of stopcocks, A, B, C, D, and E, it is possible to admit carbon tetrachloride vapor or hydrogen gas from UH_3 into the capillary tube, or pump it out along with any volatile reaction products. During the time the capillary is evacuated, the chlorides formed have an opportunity to sublime to the cold portion of the capillary. The temperature of the reaction is maintained by the nickel furnace, which is wound with nichrome wire.

After the capillary was pumped out and heated to 200°C to remove any NH_4Cl (none noted), CCl_4 vapor was admitted and the temperature raised slowly to 400 to 420°C. Chlorination was facilitated by pumping out and admitting fresh CCl_4 vapor every 10 to 15 min. The $PaCl_5$ sublimate was observed to be white. The furnace was then cooled, and the nonvolatile material at the closed end of the capillary was sealed off.

In order to reduce $PaCl_5$ to $PaCl_4$, the reaction furnace was first placed above the $PaCl_5$ sublimate and heated to 800°C. Hydrogen gas from the UH_3 furnace at 350° was then admitted to the capillary. The reaction furnace was moved slowly down toward the compound and eventually over it, thereby entrapping and forcing the highly volatile pentachloride to pass through a heated zone containing hydrogen. It took about 15 minutes to move the furnace to the end of the capillary. The furnace was then cooled down to 500°C and moved up slowly, while the system was pumped out to collect the diffuse greenish-yellow $PaCl_4$, which sublimes at 400°C in vacuum. The furnace was then cooled down to seal off the capillary from the vacuum system. An x-ray-diffraction pattern of the final product showed a tetragonal structure with a = 8.377 A and c = 7.482 A, in agreement with Fried and Zachariasen's value for $PaCl_4$.

Unit cell constants for actinide tetrachlorides are shown in Table II.

Table II

Unit cell constants for actinide tetrachlorides

Compound	a_1 (angstroms)	a_3 (angstroms)
$ThCl_4$	8.490 ± 0.001	7.483 ± 0.001
$PaCl_4$	8.377 ± 0.004	7.482 ± 0.004
UCl_4	8.303 ± 0.001	7.483 ± 0.001
$NpCl_4$	8.27 ± 0.01	7.48 ± 0.01

C. Single-Crystal Preparation

The capillary containing $PaCl_4$ was broken in vacuum by using a stopcock on a quartz tube as shown in Fig. 12a. A piece of the Cs_2ZrCl_6 matrix crystal and some glass wool were put into the tube previously. After breaking the capillary, the end of the quartz tube was sealed off and the volatile $PaCl_4$ was sublimed out to the middle part of the quartz tube as shown in Fig. 12b. The end of the quartz tube containing the capillary was then sealed off, and hydrogen gas was admitted to the tube to ~200 mm pressure. The tube was then sealed from the vacuum system, attached to a hanger (Fig. 12c), and put into the crystal-growing furnace at 900°C. The result was a homogeneous yellow crystal.

The Cs_2ZrCl_6 matrix was chosen because it cannot reoxidize Pa^{+4} to Pa^{+5}. The crystal of Cs_2ZrCl_6 was prepared by fusing stoichiometric amounts of CsCl and $ZrCl_4$ together and putting them in the crystal growing furnace at 900°C. The matrix crystal was colorless and had the K_2PtCl_6 - type cubic structure.[26] The unit cube contains four molecules with a = 10.407 A. A regular

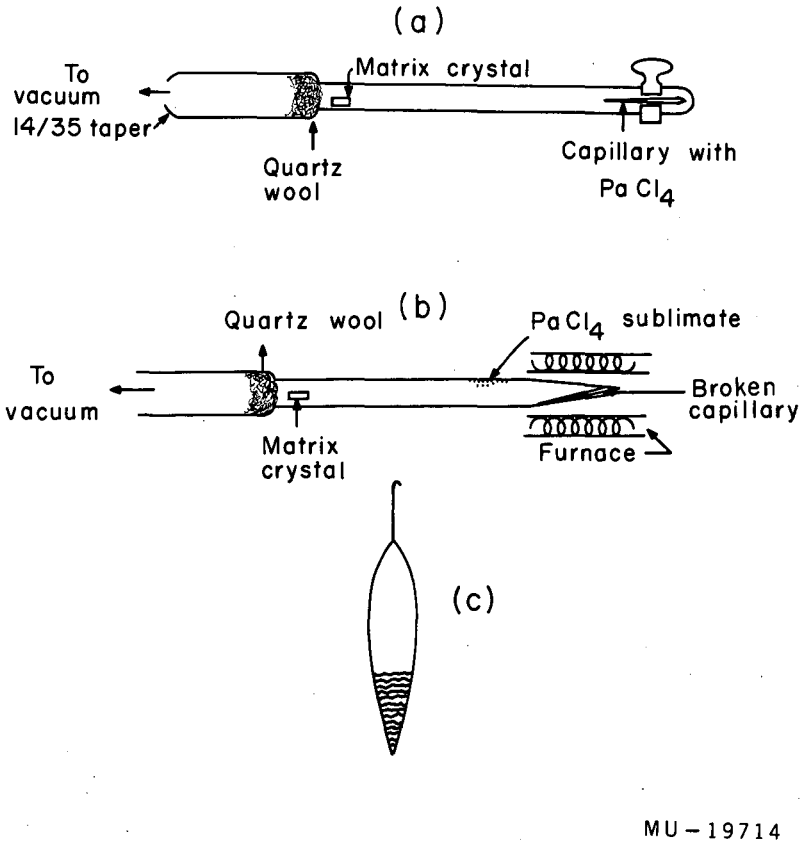

Fig. 12. Preparation of a single crystal of Cs_2ZrCl_6 containing Pa (IV). (a) Before breaking the capillary. (b) Subliming $PaCl_4$ from the broken capillary. (c) Crystal-growing tube.

octahedron of Cl atoms surrounds each Zr atom. These octahedra and the Cs atoms are distributed exactly as are the calcium and fluorine atoms in CaF_2. The Zr-Cl distance is 2.44 A.

D. Paramagnetic Resonance Measurement

The single crystal containing ~0.2% protactinium was first coated several times with Krylon to protect the reduced tetravalent protactinium from reaction with air and moisture and to prevent contamination of the paramagnetic-resonance equipment by alpha activity. The coated crystal was then put into the resonance cavity, which was surrounded by a double glass dewar filled with liquid He and liquid N_2 so that resonance measurement could be carried out at low temperatures. The spectrometer for resonance measurement has been described in Section II. D. The cavity is so constructed that the microwave H field is always perpendicular to the external magnetic field when the magnet is rotated to get different orientations of the magnetic field with respect to the crystal axis (See Fig. 13). In this way only the allowed transitions $\Delta M = \pm 1$, $\Delta m = 0$ can be measured. The frequency used was 9.447 kilomegacycles. In measurements of the external field intensity, the free-radical diphenylpicryl hydroxyl (DPH) was used as a standard. The g value of DPH is 2.004.

At liquid-N_2 temperature (77°K), no resonance line was observed, while at 4°K, four clear, nearly equally spaced lines of equal intensity were shown on the Brown recorder chart. A blank Cs_2ZrCl_6 crystal was used in place of the Pa-containing crystal, and no resonance line was observed in the same field ranges. Since the four lines from the Pa-containing crystal are equal in intensity and equal in spacing, they must be hyperfine lines corresponding to a nuclear spin 3/2. The nuclear spin assignment of 3/2 to Pa^{231} has been verified by Schüler and Gollnow,[27] and none of the possible impurities (see Table I) in Pa^{231} solution has a spin 3/2. Therefore, it is concluded that these four lines are due to Pa^{+4} (231).

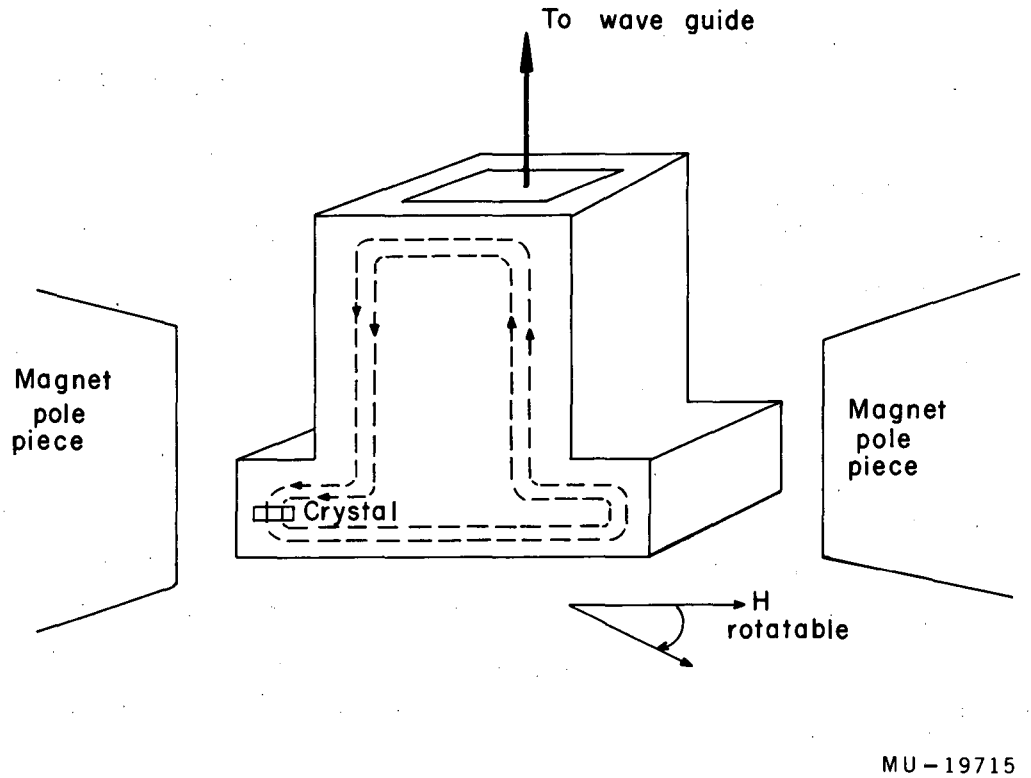

Fig. 13. Resonance cavity operating in the H_{10} mode. The magnetic field is rotable in a plane perpendicular to the wave guide.

V. RESULTS

The appearance of the four absorption lines at different orientations of the magnetic field with respect to the crystal axis is shown in Fig. 14. In Table III are listed the distances from the four hyperfine lines of Pa^{+4} to the DPH resonance line at different orientations of the magnetic field. From the average value and the small mean deviation, we may say that the absorption lines are isotropic. Using a sweep-rate of 106.7 ± 0.2 current numbers per division, we obtain the following values for the fields and current numbers of the four resonance lines and the DPH line:

	I	II	III	IV	DPH
Current No.	1640.1	1967.2	2385.1	3014.6	1270.4
Field (gauss)	4303	5075	6091	7230	3373

The current number is proportional to the magnetic current, which is in turn proportional to the magnetic field intensity except at high field intensities. The calibrated relations between magnetic field intensities and current numbers using the DPH resonance point as a standard are shown in Table IV and Fig. 15. From Fig. 15, the field intensities corresponding to the four absorption lines, are H_1 = 4303 gauss, H_2 = 5075 gauss, H_3 = 6091 gauss, and H_4 = 7230 gauss. The frequency used was ν = 9.457 kilomegacycles.

Since the spectrum is isotropic, there is no quadrupole interaction, and the spin Hamiltonian from Eqs. (3.28), (3.32), (3.33), and (3.34) can be expressed as

$$H = g\beta\vec{H}\cdot\vec{S} + A\vec{I}\cdot\vec{S} = g\beta\,[H_zS_z + H_xS_x + H_yS_y] + A[S_zI_z + S_xI_x + S_yI_y]\,. \qquad (5.1)$$

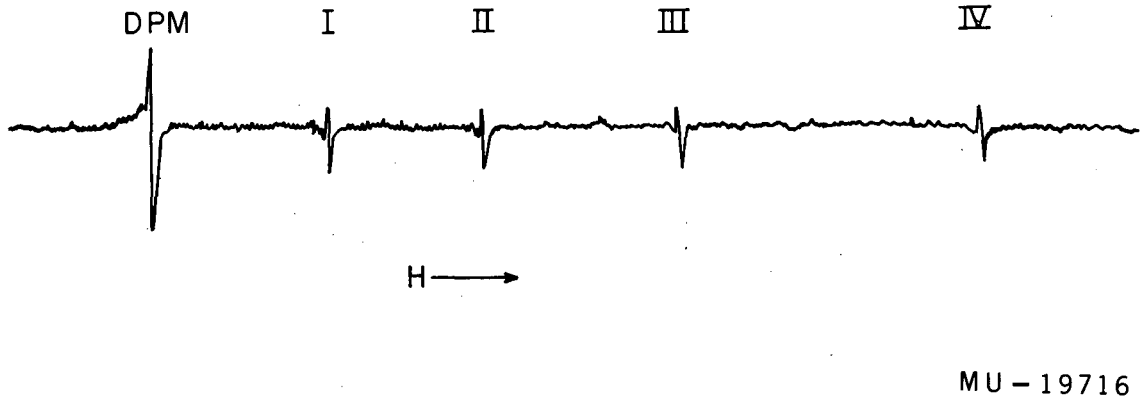

Fig. 14. Appearance of the resonance spectrum.

Table III

Positions of the four Pa^{+4} hyperfine lines

Angle (deg)	Chart divisions from DPH resonance				DPH-resonance current number
0	3.43	6.50	10.42	16.35	1274
5	3.45	6.54	10.41	16.36	1270
15	3.43	6.51	10.45	16.32	1269
25	3.45	6.53	10.45	16.33	1270
35	3.47	6.54	10.47	16.37	1273
45	3.48	6.53	10.46	16.39	1268
55	3.46	6.54	10.46	16.36	1270
65	3.46	6.52	10.43	16.30	1272
75	3.46	6.53	10.46	16.36	1270
85	3.47	6.56	10.46	16.36	1268
90	3.46	6.53	10.45	16.32	
Average	3.465	6.530	10.447	16.347	1270.4
Mean deviation	±.012	±.011	±.015	±.022	±1.6

Table IV

Relation between magnetic current, current number, and magnetic field intensity

I	Current Number	H
0.00	0000	42.6
0.10	133	397.6
0.20	269	781.0
0.30	408	1136
0.40	546	1491
0.50	671	1860
0.60	803	2229
0.70	941	2556
0.80	1074	2897
0.90	1209	3209
1.00	1345	3564
1.10	1471	3919
1.20	1611	4232
1.30	1740	4558
1.40	1876	4871
1.45	1941	4998
1.50	2008	5183
1.60	2145	5481
1.70	2280	5836
1.80	2414	6177
1.90	2550	6404
2.00	2683	6674
2.10	2825	6958
2.20	2969	7171
2.25	3037	7256
Unregulated current		
2.30		7313
2.40		7512
2.50		7739
2.60	7966	7966
2.70	8122	8122
2.80	8293	8293
2.90	8463	8463
3.02	8634	8634

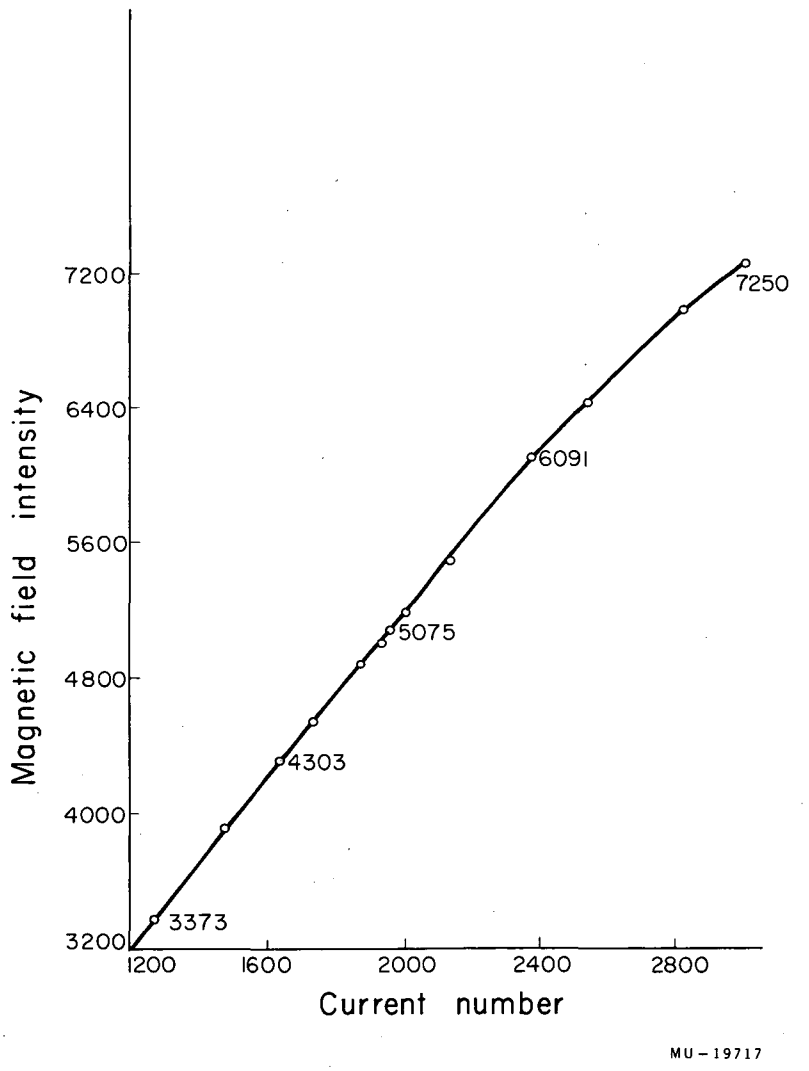

Fig. 15. Magnetic field intensity vs. current number.

For $H \parallel S_z$, let S_z be along the axis of quantization. Then we have

$$H = g\beta H S_z + A\left[S_z I_z + \frac{1}{2}\left(S_+ I_- + S_- I_+\right)\right] \qquad (5.2)$$

Simultaneous diagonalization provides the eigenvalues of the energy states of the quantum states $M = S_z = S \ldots -S$ and $m = I, I-1, \ldots -I$. If we let $G = g\beta H$, we obtain the matrix on the following page.

Let $k = M + m$.

For $k = 2$, we have

$$\left|\frac{1}{2}, \frac{3}{2}\right\rangle$$

$$\left|\frac{1}{2}, \frac{3}{2}\right\rangle \boxed{\frac{1}{2}G + \frac{3}{4}A - W} \quad ,$$

where $W = \frac{1}{2}G + \frac{3}{4}A = -\frac{1}{4}A + \frac{1}{2}\sqrt{G^2 + 4AG + 4A^2}$.

(5.3)

For $k = 1$, we can write

$$\begin{array}{cc} & \left|\frac{1}{2}, \frac{1}{2}\right\rangle \quad \left|-\frac{1}{2}, \frac{3}{2}\right\rangle \\ \left|\frac{1}{2}, \frac{1}{2}\right\rangle & \\ \left|-\frac{1}{2}, \frac{3}{2}\right\rangle & \end{array} \boxed{\begin{array}{cc} \frac{1}{2}G + \frac{1}{4}A - W & \frac{\sqrt{3}}{2}A \\ \frac{\sqrt{3}}{2}A & -\frac{1}{2}G - \frac{3}{4}A - W \end{array}} \quad .$$

From this we have

$$W^2 - \left(\frac{1}{2}G + \frac{1}{4}A - \frac{1}{2}G - \frac{3}{4}A\right)W + \left(\frac{1}{2}G + \frac{1}{4}A\right)\left(-\frac{1}{2}G - \frac{3}{4}A\right) - \frac{3}{4}A^2 = 0$$

or

$$W^2 + \frac{1}{2}AW - \frac{1}{4}G^2 - \frac{1}{2}AG - \frac{15}{16}A^2 = 0 \quad ,$$

$\lvert M, m\rangle$	$\lvert\frac{1}{2}, \frac{3}{2}\rangle$	$\lvert\frac{1}{2}, \frac{1}{2}\rangle$	$\lvert-\frac{1}{2}, \frac{3}{2}\rangle$	$\lvert\frac{1}{2}, -\frac{1}{2}\rangle$	$\lvert-\frac{1}{2}, \frac{1}{2}\rangle$	$\lvert\frac{1}{2}, -\frac{3}{2}\rangle$	$\lvert\frac{1}{2}, -\frac{1}{2}\rangle$	$\lvert\frac{1}{2}, -\frac{3}{2}\rangle$
$\lvert\frac{1}{2}, \frac{3}{2}\rangle$	$\frac{1}{2}G+\frac{3}{4}A-W$							
$\lvert\frac{1}{2}, \frac{1}{2}\rangle$		$\frac{1}{2}G+\frac{1}{4}A-W$	$\frac{\sqrt{3}}{2}A$					
$\lvert-\frac{1}{2}, \frac{3}{2}\rangle$		$\frac{\sqrt{3}}{2}A$	$-\frac{1}{2}G-\frac{3}{4}A-W$					
$\lvert\frac{1}{2}, -\frac{1}{2}\rangle$				$\frac{1}{2}G-\frac{1}{4}A-W$	A			
$\lvert-\frac{1}{2}, \frac{1}{2}\rangle$				A	$-\frac{1}{2}G-\frac{1}{4}A-W$			
$\lvert\frac{1}{2}, -\frac{3}{2}\rangle$						$\frac{1}{2}G-\frac{3}{4}A-W$	$\frac{\sqrt{3}}{2}A$	
$\lvert-\frac{1}{2}, -\frac{1}{2}\rangle$						$\frac{\sqrt{3}}{2}A$	$-\frac{1}{2}G+\frac{1}{4}A-W$	
$\lvert-\frac{1}{2}, -\frac{3}{2}\rangle$								$-\frac{1}{2}G+\frac{3}{4}A-W$

and thus

$$W = \frac{1}{4} A \pm \frac{1}{2} \sqrt{\frac{1}{4} A^2 + G^2 \pm 2AG + \frac{15}{4} A^2}$$

$$= -\frac{1}{4} A \pm \frac{1}{2} \sqrt{G^2 + 2AG + 4A^2} . \tag{5.4}$$

For $k = 0$ we obtain

$$\begin{array}{c|cc} & \left|\frac{1}{2}, -\frac{1}{2}\right> & \left|-\frac{1}{2}, \frac{1}{2}\right> \\ \hline \left|\frac{1}{2}, -\frac{1}{2}\right> & \frac{1}{2} G - \frac{1}{4} A - W & A \\ \left|-\frac{1}{2}, \frac{1}{2}\right> & A & -\frac{1}{2} G - \frac{1}{4} A - W \end{array} .$$

From this, we have

$$(W + \frac{1}{4} A)^2 - \frac{1}{4} G^2 - A^2 = 0$$

or

$$W^2 + \frac{1}{2} AW - \frac{15}{16} A^2 - \frac{1}{4} G^2 = 0$$

and thus

$$W = -\frac{1}{4} A \pm \frac{1}{2} \sqrt{4A^2 + G^2} . \tag{5.5}$$

For $k = -1$, we have

$$\begin{array}{c|cc} & \left|\frac{1}{2}, -\frac{3}{2}\right> & \left|-\frac{1}{2} -\frac{1}{2}\right> \\ \hline \left|\frac{1}{2}, -\frac{3}{2}\right> & \frac{G}{2} - \frac{3}{4} A - W & \frac{\sqrt{3}}{2} A \\ \left|-\frac{1}{2}, \frac{1}{2}\right> & \frac{\sqrt{3}}{2} A & -\frac{G}{2} + \frac{1}{4} A - W \end{array} .$$

From this, we obtain

$$W^2 - \left(\frac{G}{2} - \frac{3}{4}A - \frac{G}{2} + \frac{1}{4}A\right) W + \left(\frac{G}{2} - \frac{3}{4}A\right)\left(-\frac{G}{2} + \frac{1}{4}A\right) - \frac{3}{4}A = 0 ,$$

or

$$W^2 + \frac{1}{2}AW - \frac{G^2}{4} + \frac{1}{2}AG - \frac{15}{16}A^2 = 0 ,$$

and thus

$$W = -\frac{1}{4}A \pm \frac{1}{2}\sqrt{G^2 - 2AG + 4A^2} .$$

For $k = -2$, we obtain

$$\left|-\frac{1}{2}, -\frac{3}{2}\right>$$

$$\left|-\frac{1}{2}, -\frac{3}{2}\right> \boxed{-\frac{1}{2}G + \frac{3}{4}A - W} ,$$

where

$$W = \frac{3}{4}A - \frac{1}{2}G = -\frac{1}{4}A - \frac{1}{2}\sqrt{G^2 - 4AG + 4A^2} .$$

For $G >> A$, the different energy levels are as shown in Fig. 16. The allowed transitions have the selection rule

$$\Delta k = \pm 1, \text{ or } \Delta M = \pm 1, \Delta m = 0.$$

The four transition energies can then be obtained:

$$W_{(2 \leftrightarrow 1)} = \frac{1}{2}\sqrt{G^2 + 4AG + 4A^2} + \sqrt{G^2 + 2AG + 4A^2} \tag{5.8}$$

$$W_{(1 \leftrightarrow 0)} = \frac{1}{2}\sqrt{G^2 + 2AG + 4A^2} + \sqrt{G^2 + 4A^2} \tag{5.9}$$

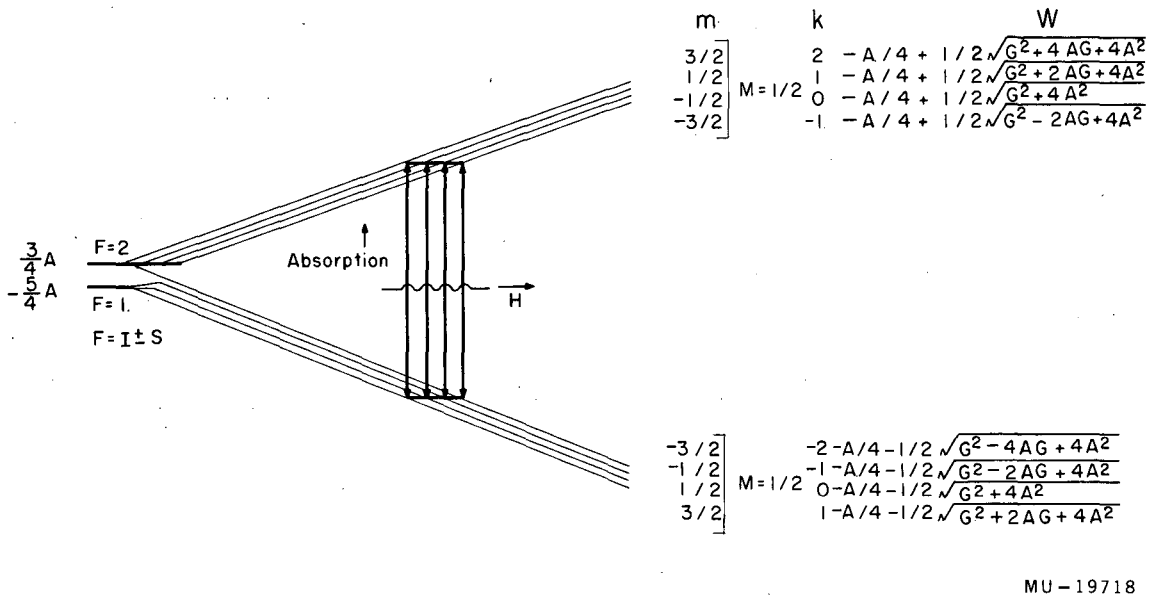

Fig. 16. Hyperfine lines and energy levels in the magnetic field.

$$W_{(0 \leftrightarrow -1)} = \frac{1}{2} \sqrt{G^2 + 4A^2} + \sqrt{G^2 - 2AG + 4A^2} \tag{5.10}$$

$$W_{(-1 \leftrightarrow -2)} = \frac{1}{2} \sqrt{G^2 - 2AG + 4A^2} + \sqrt{G^2 - 4AG + 4A^2} \quad . \tag{5.11}$$

Let $\phi = A/g\beta$. Multiplying Eqs. (5.8) to (5.11) with $2/g\beta$, we obtain

$$2\left(\frac{W_{2 \leftrightarrow 1}}{g\beta}\right) = \Gamma_1 = 2\phi + H_1 + \sqrt{H_1^2 + 2\phi H_1 + H\phi^2} \ , \tag{5.12}$$

$$2\left(\frac{W_{1 \leftrightarrow 0}}{g\beta}\right) = \Gamma_2 = \sqrt{H_2^2 \mp 2\phi H_2 \mp 4\phi^2} + \sqrt{H_2^2 + 4\phi^2} \ , \tag{5.13}$$

$$2\left(\frac{W_{0 \leftrightarrow -1}}{g\beta}\right) = \Gamma_3 = \sqrt{H_3^2 + 4\phi^2} + \sqrt{H_3^2 - 2\phi H_3 + 4\phi^2} \ , \tag{5.14}$$

and

$$2\left(\frac{W_{-1 \leftrightarrow -2}}{g\beta}\right) = \Gamma_4 = H_4 - 2\phi + \sqrt{H_4^2 - 2\phi H_4 + 4\phi^2} \ , \tag{5.15}$$

where H_1, H_2, H_3, and H_4 are the magnetic field intensities observed for the four hyperfine lines. Since $W_{2 \leftrightarrow 1}$, $W_{1 \leftrightarrow 0}$, $W_{0 \leftrightarrow -1}$, and $W_{-1 \leftrightarrow -2}$ should all be equal to the fixed resonance frequency, $h\nu$ Γ_1, Γ_2, Γ_3, and Γ_4 should all be equal.

Substituting H values into Eqs. (5.12) to (5.15), we have:

$$\Gamma_1 = 2\phi + 4.303 + \sqrt{(4.303)^2 + 8.606\phi + 4\phi^2}$$

$$= 2\phi + 4.303 + \sqrt{18.5158 + 8.606\phi + 4\phi^2}$$

$$\Gamma_2 = \sqrt{(5.075)^2 + 10.150\phi + 4\phi^2} + \sqrt{(5.075)^2 + 4\phi^2}$$

$$= \sqrt{25.7556 + 10.150\phi + 4\phi^2} + \sqrt{25.7556 + 4\phi^2}$$

$$\Gamma_3 = \sqrt{(6.091)^2 + 4\phi^2} + \sqrt{(6.091)^2 - 12.182\phi + 4\phi^2}$$

$$= \sqrt{37.1003 + 4\phi^2} + \sqrt{37.1003 - 12.182\phi + 4\phi^2}$$

$$\Gamma_4 = 7.230 - 2\phi + \sqrt{(7.230)^2 - 14.46\phi + 4\phi^2}$$

$$= 7.230 - 2\phi + \sqrt{52.2729 - 14.46\phi + 4\phi^2} .$$

In order to solve the above four equations, a curve of Γ vs ϕ for each equation is plotted as shown in Fig. 17. At a ϕ value of 0.972, Γ_1, Γ_2, Γ_3, and Γ_4 are most nearly equivalent. The average $\overline{\Gamma}$ value is 11.761.

From Eqs. (5.12) to (5.15), we have

$$h\nu = W = \frac{1}{2}\,\overline{\Gamma}\,|\,g\,|\,\beta ,$$

and hence

$$|g| = \frac{2hV}{\overline{\Gamma}\,\beta} = \frac{2\times 6.6252\times 9.457\times 10^{-18}}{11.761\times 0.92732\times 10^{-17}} = 1.148\ (\pm .005).$$

and

$$|A| = \phi g\beta = 0.972\times 1.148\times \frac{9.92732\times 10^{-17}}{6.6252\times 2.9979\times 10^{-17}}\ \text{cm}^{-1}$$

$$= 0.0529 \pm 0.0003\ \text{cm}^{-1} .$$

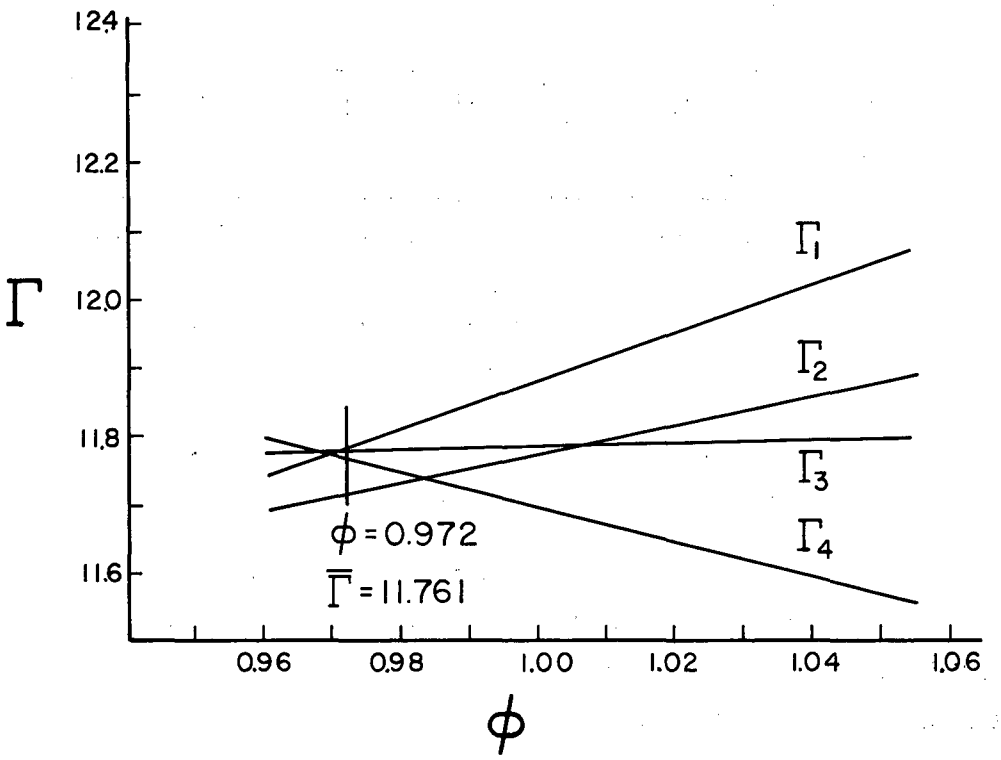

MU-19719

Fig. 17. Plot of Γ vs ϕ.

The uncertainties estimated from the accuracy of the field measurements are ~ 1/2%.

VI. DISCUSSION

No resonance was observed at 77°K. The resonances have a half-width of about 30 gauss at 4°K. No chlorine hyperfine structure was observed. Hutchison observed hperfine structures due to F in the spectra of NpF_6.[2] Presumably these are due to stronger interaction of F atoms than Cl atoms, indicating that there are π bonds in the NpF_6 complex. According to the theory developed by Griffiths and Owen and by Stevens, the magnetic electrons move partly in orbits round the central Np nucleus and partly in $P\pi$ orbits around the outer F nuclei of the complexes.[28] The hyperfine structures from florine were thus observed.

The spectra are isotropic to within the accuracy of the field measurements (~0.5%). The absolute g value obtained is 1.148 ± 0.005. These features can be most plausibly explained as arising from a single unpaired 5f electron situated at the center of a regular octahedron formed by six negative ligands, the chloride ions. The lowest energy level, as described in Section III. C transforms according to the doubly degenerate Γ_7 representation of the cubic double group. In the case of a d' electron such isotropic splitting in a magnetic field could occur only accidentally. From Section III. D, a 6d' configuration is expected to give rise to a four-fold degenerate, nonparamagnetic lowest level in a field of octahedral symmetry, or an anisotropic doublet if distortion is present.

The sign of the g value is not determined. From Fig. 18 and Eqs. (3.62), (3.63), (3.64), and (3.65) we can obtain the corresponding alpha values which are the ratios of the spin-orbit coupling to the crystalline-field splitting,

$$\frac{\zeta}{E(\Gamma_5) - E(\Gamma_2)} .$$

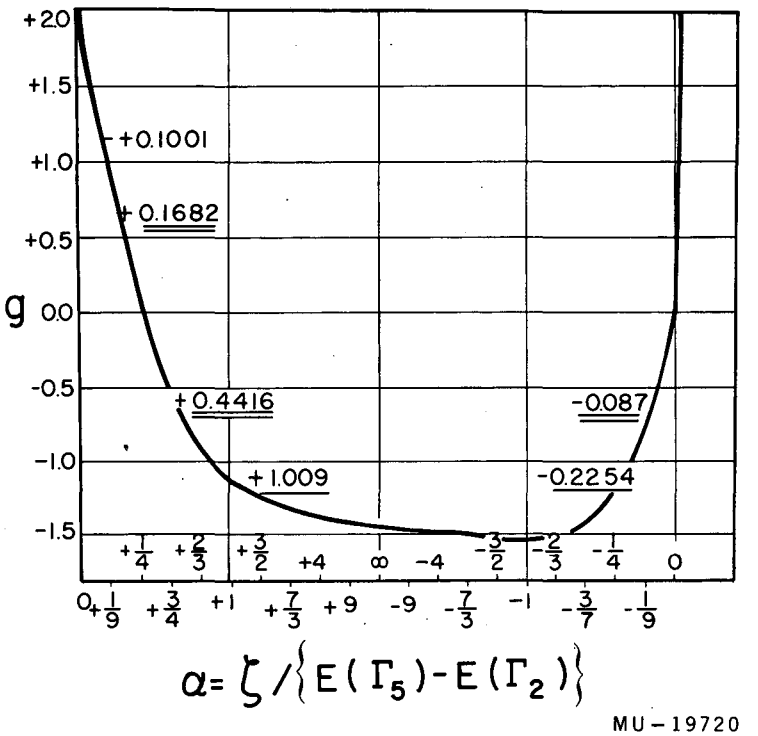

Fig. 18. Plot of g vs α. Underlined values are for $PaCl_4$; those with double underline are for NpF_6.

For $g = +1.148$, we have $\alpha = +0.1001$; for $g = -1.148$, $\alpha = +1.009$ or -0.2254. Hutchison has measured the resonance of NpF_6 and obtained $g = -0.604$, which corresponds to $\alpha = 0.4416$ and -0.087.[2] From the optical absorption data he concluded that the value $\alpha = +0.4416$ is more reasonable. The spin-orbit coupling constant ζ should be approximately the same in both Pa^{+4} and Np^{+6}, while the electric-field splitting due to fluorine will be stronger than that from chlorine. That is, $|E(\Gamma_5) - E(\Gamma_2)|$ in NpF_6 is greater than in $PaCl_6^{=}$, and therefore $PaCl_6^{=}$ should be expected to have an alpha value larger than that of NpF_6. Hence, the more reasonable value of α for $|g| = 1.148$ of the Pa^{+4} crystal studied will be 1.009.

Hutchison gave $1/hc\,(\zeta) = 2447\ cm^{-1}$, and thus $[E(\Gamma_5) - E(\Gamma_2)]/hc \cong 2447\ cm^{-1}$. An optical absorption study of Pa^{+4} in a cubic crystal has not yet been made. Its investigation should provide a basis for the verification and amplification of the above conclusions.

ACKNOWLEDGMENTS

I am greatly indebted to Professor B.B. Cunningham, under whose guidance this work has been done. His thoughtful advice and encouragement were indispensable. I wish to express my gratitude to Mr. J.D. Axe, a fellow graduate student, for his liberal cooperation in accomplishing this work and publishing the results. I am very thankful to Dr. S. Fried and Dr. J.C. Wallmann for valuable advice in the purifications and preparations of the Pa^{231} samples. I would like to thank Professors W.D. Gwinn, R.J. Myers, and C.D. Jeffries for advice in microwave-spectroscopic techniques. The resonance spectra were kindly measured by Mr. H. Stapleton. I wish to thank Mr. G. Shalimoff for running the spectroanalysis of the Pa^{231} solutions, and Miss L. Goda for her assistance in obtaining some necessary equipment. The advice and help of many members of the Lawrence Radiation Laboratory staff are greatly appreciated.

I am deeply grateful to the Lawrence Radiation Laboratory for the research assistantship under which most of this work was accomplished.

This work was done under the auspices of the U.S. Atomic Energy Commission.

REFERENCES

1. S.N. Ghosh, W. Gordy, and D.G. Hill, Phys. Rev. 96, 36 (1954); C.A. Hutchison, Jr., P.M. Llewellyn, E. Wong, and P. Dorain, Phys. Rev. 102, 292 (1956); B. Bleaney, P.M. Llewellyn, and D.A. Jones, Proc. Phys. Soc. (London) 69B, 858 (1956).
2. C.A. Hutchison, Jr., and B. Weinstock, J. Chem. Phys. 32, 56(1960).
3. B. Bleaney, P.M. Llewellyn, M.H.L. Pryce, and G.R. Hall, Phil. Mag. 45, 991 and 992 (1954); C.A. Hutchison, Jr. and W.B. Lewis, Phys. Rev. 95, 1096 (1954).
4. M. Abraham, B.B. Cunningham, C.D. Jeffries, R.W. Kedzie, and J.C. Wallmann, Bull. Am. Phys. Soc., Ser. II, 1, 396 (1956); P. Fields, A. Friedman, B. Smaller, and W. Low, Phys. Rev. 105, 757 (1957).
5. B. Bleaney, W. Hayes, and P.M. Llewellyn, unpublished data.
6. D.J.E. Ingram, Spectroscopy at Radio and Microwave Frequencies (Butterworth's Scientific Publications, London, 1955).
7. J.H. Van Vleck, Phys. Rev. 74, 1168 (1948).
8. B. Bleaney and K.W.H. Stevens, Repts. Progr. in Phys. 16, 108 (1953); A. Abragam and M.H.L. Pryce, Proc. Roy. Soc. (London) A205, 135 (1951).
9. E.U. Condon and G.H. Shortley, The Theory of Atomic Spectra (Bradford and Dickens, Cambridge, 1953).
10. M.H.L. Pryce, Proc. Phys. Soc. (London) A63, 25 (1950).
11. R.J. Elliott and K.W.H. Stevens, Proc. Phys. Soc. (London) 64, 205, 932 (1951); ibid 65, 370 (1952); Proc. Roy. Soc. (London) A215, 437 (1952); A218, 533, 219, 387 (1953).
12. A. Abragam and M.H.L. Pryce, Proc. Roy. Soc. (London) A206, 73 (1951); H.A. Bethe, Ann. Phys. 3, 133 (1929); J.H. Van Vleck, Theory of Electric and Magnetic Susceptibilities, (Clarendon Press, Oxford, 1935); R. Schlapp and W.G. Penny, Phys. Rev. 42, 666 (1932).

13. L. Pauling, The Nature of the Chemical Bond (Cornell University Press, New York, 1939); J.H. Van Vleck, J. Chem. Phys. 3, 807 (1935); J. Howard, J. Chem. Phys. 3, 813 (1935).

14. K.W.H. Stevens, Proc. Phys. Soc. (London) 65, 209 (1952).

15. E. Glückauf and H.A.C. McKay, Nature 165, 594 (1950); Leonard I. Katzin, Nature 166, 605 (1950).

16. Masso Kotani, J. Phys. Soc. Japan 4, 293 (1949).

17. H.A. John and E. Teller, Proc. Roy. Soc. (London) A161, 220 (1937).

18. K.W.H. Stevens, Proc. Roy. Soc. (London) 219, 542 (1953).

19. J.H.E. Griffiths, J. Owen, and I.M. Ward, Proc. Roy. Soc. (London) 219, 526 (1953).

20. B. Bleaney, Proc. Phys. Soc. (London) 63, 407 (1950).

21. K.A. Kraus and G.E. Moore, J. Am. Chem. Soc. 72, 4293 (1950).

22. K.A. Kraus and G.E. Moore, J. Am. Chem. Soc. 73, 2900 (1951).

23. K.A. Kraus and G.E. Moore, J. Am. Chem. Soc. 77, 1383 (1955).

24. D. Strominger, J.M. Hollander, and G.T. Seaborg, Table of Isotopes, Revs. Modern Phys. 30, 2, 585 (1958).

25. W.H. Zachariasen, Acta Cryst. 2, 388 (1949); G. Bouissieres and M. Haissinsky, J. Chem. Soc. (London), Supplementary Issue No. 2 - S256 (1949); R. Elson in Summary Report for October, November, and December, 1948, ANL-4252, February 17, 1949, p. 9, R.C.L. Mooney, Acta Cryst. 2, 189 (1914); R. Elson, S. Fried, A. Sellers, and W.H. Zachariasen, J. Am. Chem. Soc. 72, 5991 (1950); A. Sellers, S. Fried, E. Elson and W.H. Zachariasen 76, 5935 (1954).

26. R.W.G. Wyckoff, Crystal Structure (Interscience Publishers, Inc., New York, 1948).

27. H. Schüler and H. Gollnow, Naturwiss, 22, 511 (1934).

28. K.W.H. Stevens, Proc. Roy. Soc. (London) A219, 542 (1953). J.H.E. Griffiths and J. Owen, Proc. Phys. Soc. (London) A65, 951 (1952).

This report was prepared as an account of Government sponsored work. Neither the United States, nor the Commission, nor any person acting on behalf of the Commission:

A. Makes any warranty or representation, expressed or implied, with respect to the accuracy, completeness, or usefulness of the information contained in this report, or that the use of any information, apparatus, method, or process disclosed in this report may not infringe privately owned rights; or

B. Assumes any liabilities with respect to the use of, or for damages resulting from the use of any information, apparatus, method, or process disclosed in this report.

As used in the above, "person acting on behalf of the Commission" includes any employee or contractor of the Commission, or employee of such contractor, to the extent that such employee or contractor of the Commission, or employee of such contractor prepares, disseminates, or provides access to, any information pursuant to his employment or contract with the Commission, or his employment with such contractor.